Hybrid Charging Station for Autonomous Robot Using Real Time Kinematics

By

Linda Otoo

Submitted to the Department of Electrical Engineering, Electronics, Computers and Systems
In partial fulfillment of the requirements for the degree of
Master in Electrical Energy Conversion and Power Systems
at the
UNIVERSIDAD DE OVIEDO
July 2024

Author………………………………LINDA OTOO

Certified by…………….……………………………………………………

Jorge García García
Full Professor
Thesis Supervisor

Certified by…………….……………………………………………………

Jose María Holassian Mucci
Company Coordinator
Thesis Supervisor

Hybrid Charging Station for Autonomous Robot Using Real Time Kinematics

By

Linda Otoo

Submitted to the Dept. of Electrical, Electronics, Computers and Systems Engineering
On July 26th, 2024, in partial fulfillment of the requirements for the degree of
Master of Science in Electrical Energy Conversion and Power Systems

Abstract

Autonomous robot technology has been the focus in most industries in recent times. The applications of these intelligent robots extend to offices, industries, remote areas, warehouses and many more. Since they operate without human intervention, the availability of charging stations for recharging their energy is a necessity especially in remote areas.

Considering that renewable energy generation such as photovoltaic (PV) system and wind energy are set up in remote areas, monitoring of the site by individuals is a problem that needs resolution. Moreover, moving from the office to remote areas to detect faults can be tedious.

The motivation behind the thesis is to analyze, design and build a wireless hybrid PV-based charging station for autonomous robots performing tasks in remote solar panel farms.

The first step is to analyze and classify the necessary components to be used for the wireless Charging station by defining equations for estimating voltage and power capacities of them. Second step covers selection of commercially available devices based on the parameters determined during the initial stage. Next step, the third one, is to design a debugging platform using Altium designer. A PCB is designed and assembled for light indications and pushbutton operation controlled by the GPIO pins of the Nvidia Jetson Nano. The Jetson Nano is programmed in python language to implement the relevant concept. Finally, the fourth and last step consists of experiments and validation of the built circuit board together with the code programmed on the Jetson Nano.

Thesis Supervisor: Jorge García García
Title: Full Professor

Acknowledgements

I am deeply grateful to the almighty God for guiding me through this stage of my life. I also extend my heartfelt thanks to my father, who has been a role model and a source of motivation for my success. To my mother, who has been my pillar of strength, I am truly thankful. May my achievements always serve as a small token of repayment for the sacrifices they made to help me become who I am today.

To my honorable supervisor and teacher, Prof. Jorge Garcia, I appreciate him for his dedication, time sacrificed, and knowledge impacted in me to ensure that my project and studies in general were successful. His recognition and trust in my learning abilities made it possible for me throughout my studies. For the opportunities he provided for me, I dedicate this art of work to him.

I would like to express my gratitude to the organizers of the “Learn African Scholarship” in collaboration with the University of Oviedo for giving me the lifetime opportunity to pursue my dream of becoming an accomplished female engineer. I am forever indebted to you. Thank you for believing in me and sponsoring my master’s degree.

I am thankful to Prof. Sarah Saeed for simplifying my laboratory work by sharing her experiences. Her feedback and praise on my work motivated me to strive for more. Her advice and guidance throughout this thesis have been invaluable.

To the Master’s Degree coordinators, Prof. Pablo Arboleya, Prof. Jorge Garcia and Prof. Pablo Garcia, thank you for designing this master program with excellence as the major aim and collaborating with collective expertise and professors in the several scientific aspects. I appreciate the availability of these professors to teach and nurture me into a better version of myself in terms of engineering.

To Prof. Juan Gonzalez, I am deeply grateful for your words of encouragement during my first year of studies. Your words provided the hope and motivation I needed to persevere at that crucial moment.

I would like to extend my gratitude to all my professors throughout the master’s program. Their wealth of knowledge and experiences profoundly prepared us for greater endeavors. Each one of them laid a foundation for my growth, and I couldn't have come this far without their support.

To my partner, George Owusu Duah, may God bless him for the support he provided. I am grateful for his unwavering belief in me and for being my strength whenever I needed it.

Table of Contents

List of Figures

List of Tables

Chapter One

1. Introduction

1.1 Background

Renewable energy technologies like wind and solar systems have garnered significant attention since the mid-19th century. Solar energy is one of the renowned renewable energy sources. Solar PV systems are combined with several converters, battery and inverters [1]. However, these distributed generation (DG) systems are typically installed in remote locations and monitored by operators in control rooms. The distant placement of solar photovoltaic (PV) and wind energy farms necessitates regular inspections of individual substations to ensure their safe operation.

In contrast, sending technicians and engineers to remote areas for inspections is both tedious and inefficient, as it consumes time and energy (with vehicle usage contributing to energy consumption). This issue has led to the introduction of autonomous robots in workplace activities. Autonomous robots are machines equipped with sensors and processors that can process information, sense their environment, and perform complex tasks without human intervention [2]. The number of autonomous robots is steadily increasing as they are integrated into various technical fields, including manufacturing and self-assistance. In each of these areas, they play a crucial role by addressing significant challenges [3] faced by workers in accessing specific information and data for analysis.

The idea of intelligent robots with independent arm movement commenced about eighty years ago during World War II. Advancement in computer sciences and electronics with upgrades in mechanical engineering made this idea possible to be shaped [4]. Research and development in mobile robotics have been a major focus for eight decades now. In these contemporary times, [4] combination of robotics and artificial intelligence has been solid, concentrating on providing robots with the ability of making unsupervised decisions similar to human recognition. These intelligent, self-decision-making robots have the potential to revolutionize human capabilities and significantly enhance our intelligence. In several physical service sectors such as cleaning, security, and tasks that do not require creative or analytical thinking, these robots can efficiently perform assigned duties. Additionally, they could play a crucial role in military operations, potentially reducing the need for human involvement in warfare [4]. Autonomous robot applications are on the rise in most industries, specifically in electric vehicle autonomous charging.

Considering this technology, wind farms and PV farms can make use of them in the remote areas where renewable generation systems are established. In order to guarantee human-free intervention of robot operation, there should be availability of remote charging stations for robots to recharge and continue their daily activities. [5]They have the intellectual capacity to move autonomously without encountering obstacles in their operational surroundings. They employ sensor technologies to detect their environment and carry out their designated tasks [6]. Due to the stated characteristics of intelligent robots, they are capable of functioning in a Solar PV farm. In the PV farm, they are utilized to monitor the panels. Using artificial intelligence with the robots, a live view of occurrence in the farm is seen by operators in the control room. To ensure this independent activity, a standalone charging station needs to be available within the reach of robots for recharging when they run on low battery. The proposed charging station must have uninterrupted communication with the self-reliant robot since they use tracking methods to locate a specific point.

This thesis addresses the design and construction of hardware setup of a wireless hybrid charging station using solar PV, Battery Energy Storage System, programming of Nvidia Jetson Nano A206 for communication with inverter/ simpleRTK2B and other peripherals in the topology and design of the debugging pushbuttons (PCB design and building) based on the energy consumption of Bunker Mini robot.

The undertaken topology is a standalone wireless hybrid PV-Battery energy storage (BESS) charging station. This technology consists of 1kW, 12Vdc-230Vac MPPT Solar charger inverter controller connected with 400Wp, 12V solar Panel, simpleRTK2B, Internet router and 100Ah-12V LiFePO4 battery storage used to charge the robot's battery, as well as other ancillary subsystems. Wireless charging is established between charging station and robot through transmitter and receiver respectively.

In future works, the system must be able to be scaled to include hybrid generation and storage systems (namely a small wind generator or an internal combustion engine (ICE) generator) to ensure continuity of demand supply under no sunlight circumstances.

1.2 Objectives

The central theme of this thesis is to design and construct hardware setup of the wireless charging station which is the basic definition from WICS for autonomous robots and verify its operation. The fundamental objectives guiding the work process can thus be listed to:

- Analysis of energy consumption of autonomous robots. The result of this analysis defines the operation of the converter (MPPT solar charger inverter) and correct selection of other components for the topology.

- In the first stage, selection and sizing of PV panels, Battery energy storage system, inverter and Wi-Fi. With this, proper components of correct values of voltage and power are chosen for the design.
- The system must consider hybrid generation systems and must be able to incorporate a generation technology different from PV (e.g. ICE generator or Wond generator).
- Programming of Nvidia Jetson Nano A206 GPIO's. A code is written to blink LEDs using pushbuttons (External) through the GPIO pins.
- PCB design for LEDs and Pushbuttons controlled from Jetson Nano GPIOs.
- Design of an experimental setup for the analysis and design made theoretically for testing and authentication.
- Verification of the built prototype charging station performance. During this process, expected operation of the prototype is validated compared with simulated and analysed system.

1.3 Thesis Structure

Towards the previously mentioned objectives, the thesis work was developed, and the structure is organized as follows:

Chapter1: Introduction

This present chapter elaborates on the motivation for the work carried out in this thesis. In this section, the scope of work of the project is highlighted and design architecture is clearly stated. The major objectives of the work are outlined and an overview of the layout of the thesis in chapters.

Chapter 2: Literature Review

This chapter reviews the research literature that allows entrance for the work carried out in this thesis. First of all, previous topologies of hybrid PV systems are evaluated. Secondly, there will be a need for a storage system to save energy from the PV system. In view of this, distinct battery energy storage systems are analysed to check their compatibility with PV systems. Pointing out the merits and demerits of the various categories of batteries. Thirdly, solar controller schemes are explored stating their benefits and drawbacks in the charging of batteries. Lastly, a review of charging system topologies is revealed.

Chapter 3: System Design Requirements

This chapter exhibits a detailed analysis of specifications of the individual devices used in the setup. Calculations of voltage and energy capacity needed in storage to be able to recharge the robot. Using the battery voltage and capacity, solar panel power rating is selected based on the limited requirements provided by the company. Moreover, with the parameters of the solar panel, the necessary power rating of solar charger controller is required to perform efficiently its functions. The chapter concludes with known values of voltage, power and energy of battery, solar inverter, solar panels necessary for the proposed design.

Chapter 4: Selection of Components

This chapter captures exploring of commercially available devices based on the analysis made in **chapter 3**. In this chapter, several options of peripherals from different companies are searched and investigated to ensure that it suits the already provided components such as the Jetson Nano, Real time kinematics (RTK simple) and the wireless connectors.

Chapter 5: Architecture and Schematic of Proposed Design

In this chapter, the schematic of proposed charging station design is illustrated with description of each component and their function. Architectural design of structure of the charging station and detailed discussion is scripted on it.

Chapter 6: Development and Control of Debugging Platform

This chapter designs a PCB for LED indications controlled by pushbuttons by code programmed on the Nvidia Jetson Nano A206 using Python program. The LED and pushbutton circuits used in the printed circuit board are illustrated in figures. Calculations made to single out resistors, transistors, LEDs, capacitors and pushbuttons for this application are elaborated. Figures displaying the schematic of the circuit and PCB design are included.

Chapter 7: Experiment and Results

This chapter captures the testing and analysis of the results for the PCB design. A test made on breadboard is shown as well as validation of the printed circuit board. Results are vividly explained and discussed in detail.

Chapter 8: Conclusions and Outlook

This chapter indicates the conclusions reached out of the thesis work and outlooks a future path for research in this field.

Chapter Two

2. Literature Review

The chapter is structured as follows:

- First, an in-depth analysis of existing hybrid PV charging stations is conducted. The study also evaluates previous research works on solar panel-powered charging stations done by other authors.
- Secondly, a comprehensive review is conducted on battery energy storage systems suitable for PV installations, focusing on their durability in outdoor conditions. This research examines the features of different battery types.
- Thirdly, an analysis is conducted on commercially available solar charger controllers, discussing their benefits, drawbacks, and uses.

The review is then assessed in answer to the requirements of the application under study.

2.1 Existing Hybrid Charging Stations

This section investigates various hybrid charging stations that are currently in use. The different areas where these systems are applied are steadily reviewed.

2.1.1 Standalone PV Charging System for Acid Battery

In [7] , a standalone solar energy battery charger for a 40Ah, 48V lead acid battery system incorporated with Pulse width modulation (PWM) based voltage-controlled boost converter was designed and simulated using MATLAB. The proposed design was limited to dc applications. Figure 1 illustrates the proposed project by the authors. Lead acid battery bank is being recharged by solar PV panels through controlled boost converter.

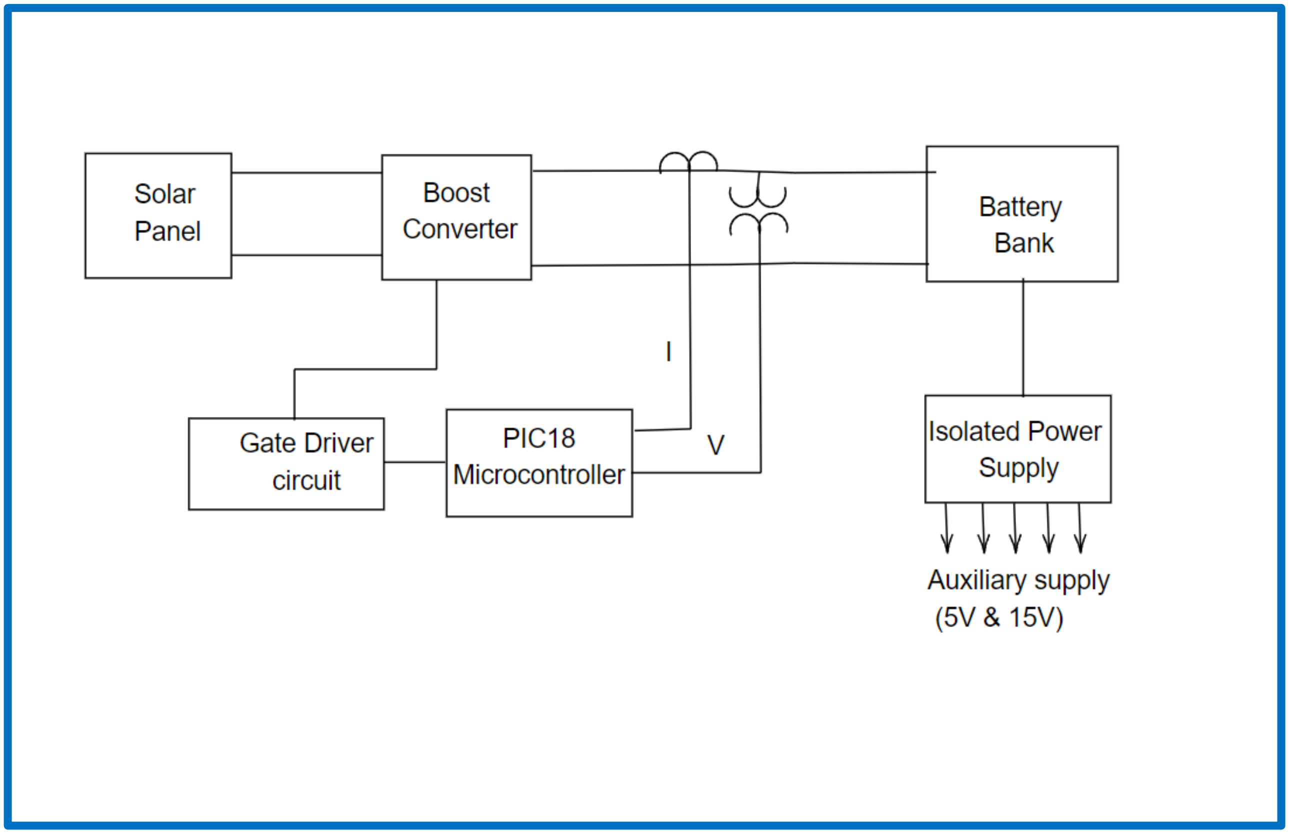

Figure 1: Block diagram of proposed design [7]

Boost converter increases voltage level of the PV output to charging voltage value. The PWM boost converter operates based on voltage mode control principles to regulate both output voltage and current for effective battery charging control. Since the project operates independently as a charging system, all necessary auxiliary power for different components and circuits is sourced from an isolated power supply specifically designed to provide consistent 5V and 15V outputs at 1 ampere.

2.1.2. Standalone Solar PV Electric Vehicle Charging Station

Reference [8] performed a case study in India. The authors of this paper designed and analysed a standalone solar PV charging station for an electric vehicle. A 30 W standalone PV based EV charging station was modelled with a one-day backup. In addition, controllers needed to reinstate DC bus voltage and regulate charging and discharging of storage batteries. System validation was done using MATLAB/Simulink.

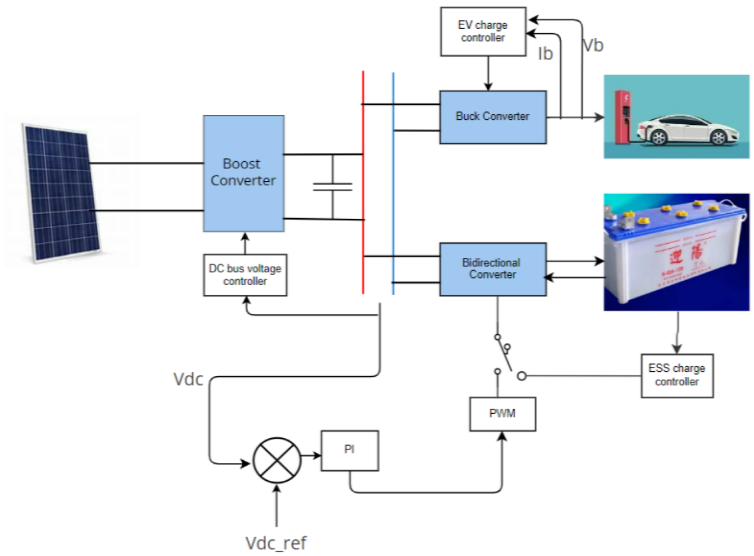

Figure 2: PV powered EV charging Station [8]

2.1.3. Low Operation Cost Hybrid Charging Station for EV

This section thus presents a charging station (CS) utilizing monocrystalline solar photovoltaic (PV) array, a battery energy storage system (BESS), the grid and a diesel generator set to [9] ensure uninterrupted charging of electric vehicles (EVs). The main objective of the suggested technology is to reduce the operational cost of the charging station.

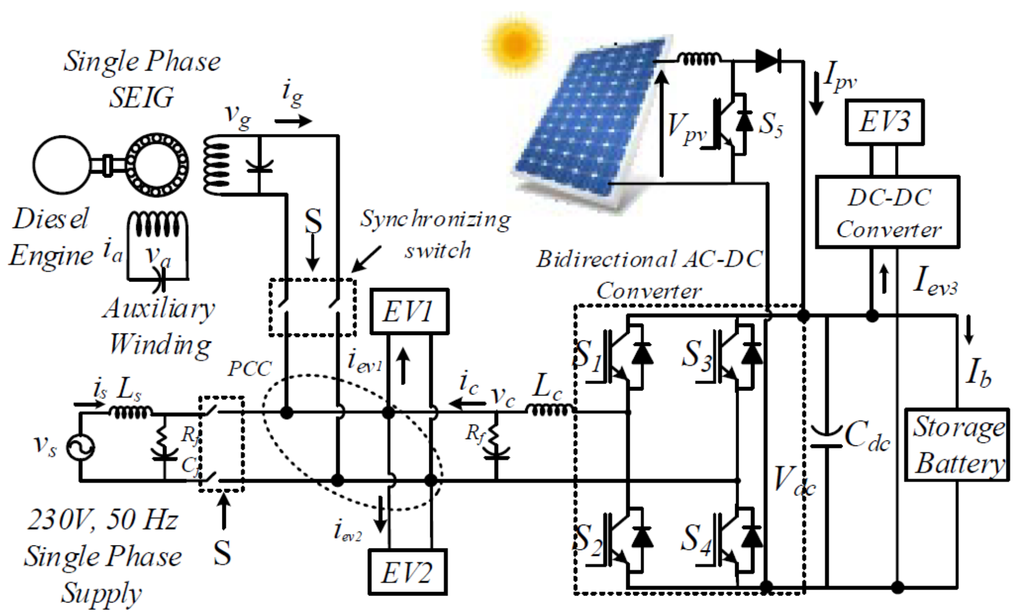

Figure 3: Topology of Hybrid Charging Station for EV [9]

The circuit topology of the suggested CS is displayed in Figure 3. As seen in Figure 3, the model includes a single phase two winding self-excited induction generator (SIEG) connected to a three-phase squirrel cage motor induction motor (SCIM), indicating a diesel engine. To ensure energy efficiency, a battery energy storage is coupled to the DC bus of the voltage source converter (VSC) using a boost converter. Since EVs require their batteries to be charged and discharged, the proposed design has a connected EV through a bidirectional boost converter to the DC bus.

Although this topology consists of lots of components which makes the capital cost quite expensive, the achieved result met validated the objectives of design with total harmonic distortion less than 5%. Moreover, this technology is only applicable for EVs and cannot be used in remote areas where the Grid is unavailable.

2.1.4. Design and Implementation of Autonomous Charging Station for Agricultural Electric Vehicles

In [10], the researchers designed and implemented a self-reliant charging station to be applied in farms to prevent farmers from following vehicles to manually connect them to the charging port. During this project, they made use of a holonomic mobile platform and a collaborative robotic arm. They presented a charging station with docking mechanism, communication techniques and utilized algorithms purposely for autonomous charging. The setup is illustrated in Figure 4.

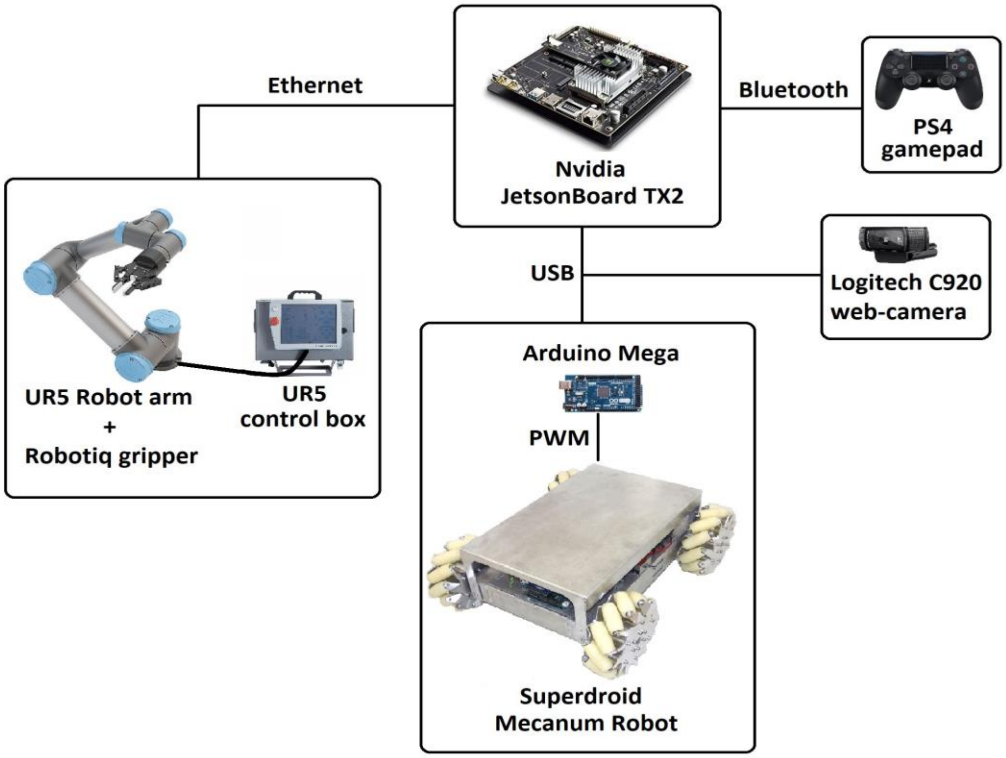

Figure 4: Global Hardware architecture of the autonomous charging station [10]

2.2. Battery Energy Storage for PV Application

This section provides investigation of appropriate battery technologies applied in solar PV hybrid installations. Battery energy storage is an essential aspect of PV systems. Aside their capacity to store electrical energy generated by PV arrays and supply when the need arises (non-sunny days and night periods), batteries are capable of stabilizing voltages by reducing fluctuations in PV systems and preventing loads from damages [11]. Furthermore, in electrical machines like motors, high starting current is required therefore the presence of battery with a PV provides aid in supplying surge currents.

The recent article [11], a summary of batteries compatible with PV systems was done. PV standalone hybrid generation systems need to save electrical energy in batteries during sun hours to enable frequent power supply to load during unstable environmental phenomenon. Depending on the project, the characteristic of the battery has to be known. Types of batteries to be considered include Lead acid (has different categories such as Gel, flooded cell, absorbed Gas Mat (AGM)), Nicke-Cadmium (Ni-Cd) batteries, Nickel-Metal hydride (Ni-MH), Lithium ion (Li-ion) batteries, and

Lithium polymer batteries in the following subsections, the characteristic of each were analysed.

2.2.1. Types of Batteries

2.2.1.1. Lead acid Batteries.

Lead acid (LA) batteries are known to be one of the most developed technologies with low self-discharge and minimal capital cost [12]. These characteristics make LA advantageous when compared with other batteries. On the contrary, [11] LA has an extremely small life cycle, energy and power density. Due to its demerits, they appear in huge sizes and relatively heavy therefore not applicable in PV-battery integrated module (PBIM). PV technologies necessitate a large energy density capacity to store enough energy during sunny hours.

2.2.1.2. Nickel Cadmium (Ni-Cd) Batteries

These batteries provide larger power, energy density and higher life cycle [13]. The presence of cadmium in Ni-Cd makes it extremely dangerous to the environment and equally generates memory effect which limits the battery's capability [14] based on its application and higher self-discharge. Memory effect is defined as the ability for a battery to recover its depth of discharge in the past.

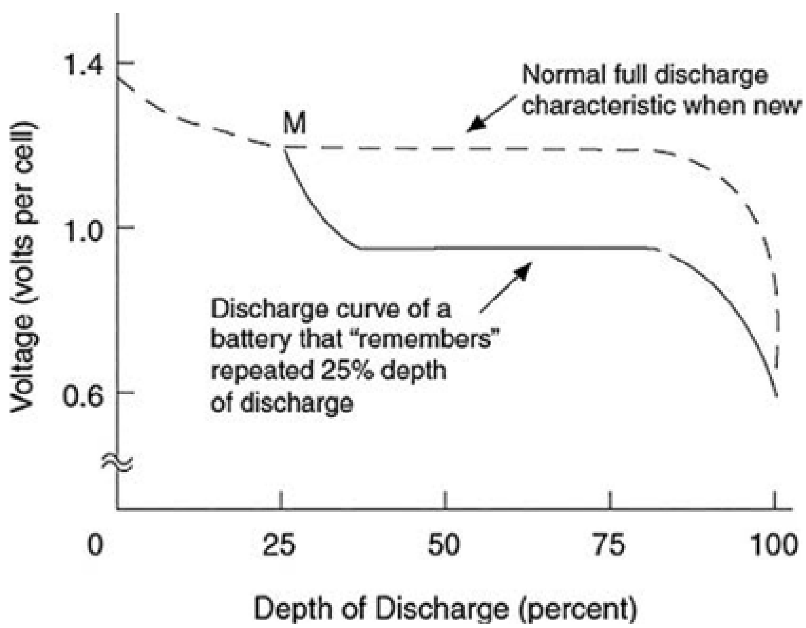

Figure 5: Memory effect of Ni-Cd battery [11]

2.2.1.3. Nickel Metal Hydride (Ni-MH)

Ni-MH battery is an upgrade of the Ni-Cd with higher energy density and contains lower memory effect [11]. It generates higher power. Overcharging damages, High cost, higher self-discharge and low efficiency are the disadvantages of Ni-MH [15].

2.2.1.4. Lithium Ion (Li-ion) Batteries

The energy density of Li-ion batteries is three times greater than that of Pb-acid batteries. The cell voltage is 3.5V and connecting a few cells in series provides the necessary battery voltage. During each discharge and charge cycle, the lithium electrode reacts with the electrolyte, forming a passivation film [11]. This issue is mitigated by using thick electrodes, which contributes to the higher cost of Li-ion batteries compared to NiCd batteries. Additionally, overcharging can damage the battery. Table 1 contains an overview of current battery technologies and their characteristics.

Therefore, Li-ion batteries emerge as a viable option for PV systems due to their higher energy density compared to lead-acid, NiCd, and NiMH batteries, along with greater efficiency. Furthermore, Li-ion cells avoid issues related to memory effect and toxic elements. However, Li-ion batteries are generally more expensive than lead-acid and NiCd batteries and are susceptible to self-discharge.

Table 1: Summary of Available Battery Technologies [12]

Type	LA	NiCd	NiMH	Li-ion	Nas	VRB
Energy density (Wh/kg)	25–50	50–60	60–120	75-200	150-240	10-30
Power density (W/kg)	75–300	~200	250-1000	500-2000	150-230	80-150
Cycle life (100% DOD)	200–1000	>1500	180-2000	1000-1000	2500-4000	>12000
Capital cost ($/kWh)	100–300	300–600	900-3500	300-2500	300-500	150-1000
Round-trip efficiency	75–85	70–75	65-80	85-97	75-90	75-90
Self-discharge	Low	High	High	Medium	-	Negligible

Lithium-ion batteries include Lithium iron phosphate (LiFePO4 or LFP), Lithium manganese oxide (LiMnO2), Lithium cobalt oxide (LCO), etc. In [16], LFP battery is realized to have stable and matured Li-ion technology. It has strong thermal stability, great power capacity and is determined to be the secured lithium-ion battery regarding thermal runaway hazard. These features make it considerable for PV applications. The only shortcoming of LiFePO4 is the lower average voltage resulting in smaller energy, but it is still capable of higher energy compared to other lithium-ion batteries [17].

2.3. Solar Charger Controller

A solar charge controller enhances the efficiency of solar power transfer to the battery. In [18], the controller regulates the charging process of the battery connected to the PV. The primary challenge in a solar charger system is keeping the DC output power from the solar panel constant.

2.3.1. PWM Solar Charger

Paper [19] presents analysis and design of solar charger controller using PWM. In this scheme, the PV system was connected to the grid hence the controller was modelled to function as an uninterruptible power supply to the connected load, regulate the charge and discharge of battery system and to ensure constant current constant voltage charging technique of the battery. The block diagram of the modelled system is outlined in Figure 6.

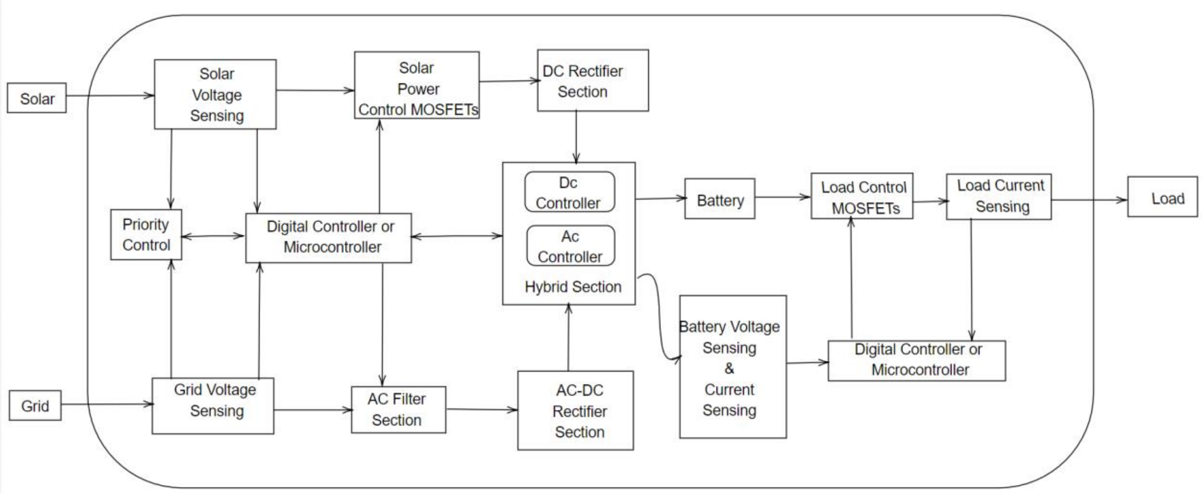

Figure 6: Developed Solar Hybrid Charge Controller [19]

2.3.2. MPPT Solar Chargers

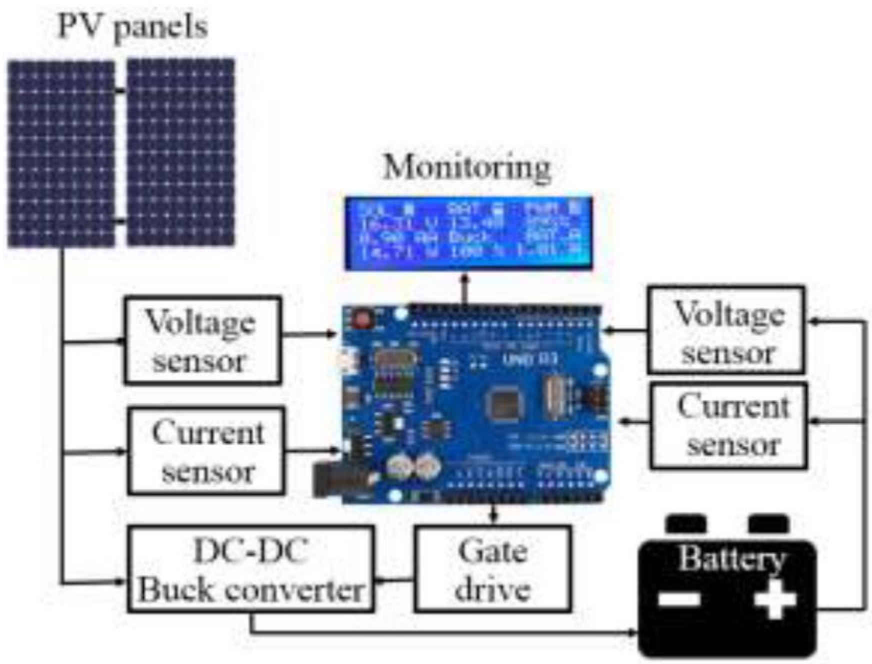

Figure 7: Structure of Experimental Setup [20]

The schematic illustrated in Figure 7 presents the schematic drawing of the experimental setup introduced by [20]. The study proposed is a design and development of PI controlled based Maximum Power Point tracking (MPPT) techniques for solar charger controllers with the aid of DC/DC buck converter. During this research, the author made use of the following peripherals: Solar Panels, DC/DC buck converter, MPPT solar charger controller using Arduino UNO-R3, 12V battery, 20x4 LCD monitoring, gate driver circuit and resistance load. The Arduino UNO-R3 was programmed for real time monitoring of the prototype output power of the PV.

In addition, researchers in [18] designed and analysed an MPPT (Perturb and Observe algorithm) charge controller. During their study, the dynamic response and control action of the PV system was validated by simulation in MATLAB/Simulink. The structure of proposed design is illustrated in Figure 7.

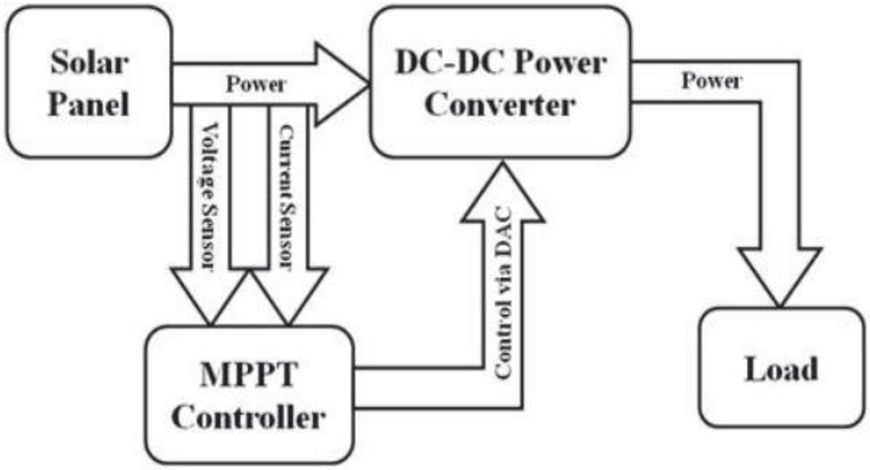

Figure 8: Basic Topology of MPPT Charge Controller [18]

The fundamental block diagram includes a PV cell, a boost converter, an inverter, and a load, as displayed in Figure 8. The PV cell captures solar energy and converts it into electrical energy. The boost converter raises the low solar voltage to a level suitable for the DC connector, which is directly connected to the monocrystalline PV cell's inverter [18]. The inverter then converts the unregulated voltage into a regulated voltage. A standalone PV of 12V and power range of (50-100) W which is capable of charging batteries during the day and used during nighttime. According to their results, this model can be implemented in a remote area.

2.4. Conclusions

This chapter has reviewed existing prototypes of PV-based Hybrid charging stations available. Moreover, different types of batteries compatible with PV system applications were investigated to determine the authentic one for an outdoor application. Considering the usage of BESS, there will be a need to recharge batteries as well as the battery of the load (Robot) in this thesis. In order to avoid overcharging of batteries, charger controllers are necessities to enable correct charging of batteries. Two options (MPPT and PWM solar charger controller) of these controllers were reviewed to detect which one provides high efficiency in terms of battery charging.

After careful evaluation, it can be concluded that using MPPT controller will always provide maximum power of the solar panel. Lithium-ion batteries were noticed to have high energy and power density compared to all other energy storages. Hence Li-ion is considered as the best storage type for PV systems.

Chapter Three

3. System Design Requirements

Through the literature review, presented in Chapter 2, it has been concluded that monocrystalline type of panel is commonly used in PV installations. Based on the energy capacity of the autonomous robots, capacity of the energy storage is estimated as well as the needed amount of power to charge the BESS. Lithium iron phosphate (LiFePO4) is selected to be the best type of lithium ion for this application due to its high thermal stability as evaluated in chapter 2. Since the proposed charging station is to be operated in an outdoor condition, all peripherals are expected to be able to withstand harsh environmental conditions.

This chapter is constructed as follows:

- First, the autonomous robot which is the considered load in this project is analysed to determine its energy capacity. Using detailed information such as energy consumption of the robot, the amount of energy needed in the battery storage is calculated to ensure continuity of power supply for the charging of the robot in the absence (at night) of the PV system. The voltage range of the BESS is equally estimated.
- Second, considering the analysed voltage and energy capacity of the BESS, the number of solar panels and total power required to charge the BESS as well as supplying the connected load is determined.
- Lastly, the power rating, voltage and current rating of solar inverter charger controller is also determined based on the power of the solar panel.

Then, in the next chapter, accessible commercial options are searched for and ordered for the hardware setup.

3.1. Autonomous robot energy consumption

The charging station is designed to supply charging power to autonomous robots. Figure 9 Figure 9 shows the image of the SCOUT 2.0 robot. The technical parameters of the robot are outlined in Table 2.

Figure 9: SCOUT 2.0

The technical specification of the load is listed in Table 2.

Table 2: Specifications of SCOUT 2.0

Parameters	**Values**
Battery type	Lithium battery
Battery voltage	24V
Battery capacity	30Ah
Power drive motor	Dc brushless 4x400 W
Weight	67kg
Battery charging time	3hours
Size	930 x 699 x 349
System Interface	CAN

From the datasheet of the device, it is seen that maximum voltage of the robot's battery is 24V with 30Ah capacity. Total energy of each robot is calculated to be $30Ah \times 24V = 720Wh$. In this project, two loads are considered, therefore, the energy storage is designed to have a capacity more than twice that of the robot.

3.2. Estimation of BESS Capacity

In reference to the data analysis made in section 3.1, BESS must be capable of supplying power to the robot with the right voltage level, thus BESS voltage is required to be 24V. As stated before, the battery capacity is estimated to be about three to four times that of robots. In that case, battery capacity is analysed to be in the range of 90-120Ah. The Table 3 below shows battery parameters estimated. Commercial options are searched for based on this design.

Table 3: BESS parameters

Parameters	Value
Voltage range	12V-24V
Capacity range	90-120Ah

3.3. Solar Panel Power Rating

To determine the power of the solar panel needed, several calculations are done as follows: In these calculations, conditions given include:

- The average hours of sunlight at the solar panel location under this study is 7 hours.
- Consider each panel's power rating between 200-250Wp. This is to aid in the selection of a reasonable panel size for the station.

3.3.1. Option one

In the first option, 12 V and 100Ah capacity of battery energy storage is contemplated.

$$Battery\ Capacity = 100Ah$$

$$Voltage\ = 12V$$

$$Average\ hours\ of\ sunlight = 7$$

$$Amper\ rating = \frac{Battery\ Capacity}{Average\ hours\ of\ sunlight} = 14.29$$

$$Number\ of\ Panels\ = \frac{Amper\ rating}{maximum\ current\ rating\ of\ the\ available\ panel} = \frac{14.29}{8.26}$$

$$= 1.73$$

Considering a solar panel with maximum current of 8.26A, 200 or 250Wp and maximum voltage of 30.3V. From the above calculation, it can be deduced that relatively two panels of 250Wp or 200Wp connected in parallel or series are capable of charging 100Ah, 12V battery. If connected in parallel, the total power from the PV will be in the range of 400-500Wp.

3.3.2.Option two

This option is used when the voltage of battery is 24 V and 120Ah capacity and using the same power rating of panels as used in option 1.

$$Battery\ Capacity = 120Ah$$

$$Voltage\ = 24V$$

$$Amper\ rating = \frac{Battery\ Capacity}{Average\ hours\ of\ sunlight} = 17.14$$

$$Number\ of\ Panels\ = \frac{Amper\ rating}{maximum\ current\ rating\ of\ the\ available\ panel} = \frac{17.14}{8.26}$$

$$= 2.08$$

Approximately 2 panels of either 200 or 250Wp connected in parallel have the capacity to charge the battery.

3.4.Battery Charging Time

Depending on the nominal voltage and maximum power of the panel, the time taken for the solar panel to charge the battery is then deduced. Under optimal conditions, panel with continuous 24V, 250Wp is capable of handling a maximum current of

$$\frac{PV\_\max\ \_Power}{Nominal\ voltage} = \frac{250 \times 2}{24} = 20.833A\ .$$

If the allowed depth of discharge of the battery is 50% and the expected maximum state of charge is 90%, it depicts that the panel has to recharge the battery of 40% value. Based on this, the time taken by the solar panel to charge the battery from 50% to 90% is calculated to be.

Battery percentage used = $40\%\ x\ 120Ah = 48Ah,$

Time taken for PV to compensate for the 48Ah =$\frac{48}{20.833} = 2.3$ hours.

If a 12V, 200Wp solar panel is used, battery charging time results to

$$\frac{PV\_\max\ \_Power}{Nominal\ voltage} = \frac{200\times2}{12} = 33.333A\ .$$

Time taken for PV to compensate for the 48Ah =$\frac{48}{33.333} = 1.44$ hours.

3.5.Solar Charger Controller

Using a solar panel power range of 400-500Wp, voltage range of 12-24V of energy storage, solar inverter controller power rating is then determined. In order to ensure that the efficiency of the system is about 50% or more, the inverter operating range is estimated between 800W to 1kW and voltage range of 12-24V.

Chapter Four

4. Selection of Components

Based on the specified values of voltage, power and energy in previous chapter, internet is searched for commercial availability of the components with the estimated parameters.

4.1. Available Commercial LiFePO4 Batteries

As stated in chapter 3, voltage range considered for this application is 12V to 24V with capacity range of 100-120Ah. Considering these values, the following are some commercial batteries searched.

4.1.1. LiFePO4 Battery by Manly

Figure 10: LiFePO4 battery from Manly [21]

This battery storage from Manly has 120Ah capacity and 24V potential. In Table 4 is a list describing its capabilities. This component has an inbuilt Battery management system (BMS) in charge of protecting the battery against overcharging, over-discharge, short circuits and over current. Some merits of the product include:

- Long lifespan beyond 10years
- Incorporated with individual cell balancing.
- Possesses high energy density.
- Easier to maintain.
- Charges faster
- Robust safety (No fire, no explosion)

Table 4: Table of Specifications of Manly LiFePO4 battery

Specifications	Values
Nominal Voltage	24V
Energy	3072Wh
Nominal Capacity	120Ah
Max. Voltage	25.6V
Life cycle	5000+
Charge temperature	0 ~ 45°C
Discharge temperature	-20 ~ 75 °C
Waterproof level	IP65
Communication protocol	RS485/RS232/CAN Bus/Optional
Battery type	LiFePO4

4.1.2. LiFePO4 Battery by KEPWORTH

From Kepworth, there existed two battery products that met the requirements: 12V,100Ah and 24V,100Ah $LiFePO_4$. Figure 11 and Figure 12 show the storage battery product from Kepworth. These batteries consist of a built-in Bluetooth and just as the one from Manly includes a BMS. Both have great safety performance and higher efficiency. Again, they have stable operation performance compared to Lead Acid Battery. Their characteristics are seen in Table 5.

Figure 11: 12V,100Ah battery storage by KepWorth [22]

Figure 12: 24V,100Ah battery storage by KepWorth [23]

Table 5: Battery Specifications

Parameters	**12V battery**	**24V battery**
Nominal voltage	12.8V	25.8V
Rated Voltage	12V	24V
Capacity	100Ah	100Ah
Operating temperature	-20 ~ 60°C	-20 ~ 60°C
Charging temperature	0-45°C	0-45°C
Lifecycle	6000 cycles –70%	4000—100% 6000—70%
Max Charge Current	1C	1C

4.1.3. LiFePO4 battery by ECGSolax

Figure 13: 12.8V,100Ah Capacity Battery by ECGSOLAX

Capacity: 100Ah (0.2C/25°C) (Min:29Ah)

Nominal Voltage: 12.8V

Operating Voltage Range: 10V~14.6V (Typical:12.8V)

Charging Voltage: 14.6V

Discharge Cut-off Voltage: 10V

Charging Current (Max.): 50A

Discharge Current (Max.): 100A

Figure 14: Battery Characteristics

The battery energy storage from ECGSOLAX contains an alarm and protection mode. This feature prevents over voltage, under voltage, over current and short circuit in the battery. In addition, it can operate in a humidity range of 15% - 85%. The image of the product and its specifications can be viewed in Figure 13 and Figure 14 respectively.

Table 6: Table of all Batteries Available

Batteries	Manufacturer	Nominal Voltage [V]	Capacity [Ah]	Operating Temperature
	Manly	24	120	-20~75°C
	KepWorth	12.8	100	-20~60°C
	ECGSolax	12.8	100	-10~75°C
	KepWorth	25.8	100	-20~60°C

Table 6 contains all battery options analysed and compared.

4.2. Available commercial Solar Panels

4.2.1. Solar Panels by Enjoy Solar Company

The solar panel designed by Enjoy solar industry has one with power of 200W and maximum power point voltage of 36.2V. Its operating temperature and power capacity make it an option for the proposed design. The datasheet of the device is summarized in Table 7 while the module layout is shown in Figure 15.

Figure 15: 200Wp, 36.2 Vmp, 5.53A Imp, 6.34A Isc Solar Panel by Enjoy Solar company

Table 7: Panel electrical parameters

Specification	Value
Rated Max. Power [W]	200
Voltage at Pmax [V]	36.2
Current at Pmax [A]	5.53
Open circuit Voltage [V]	40.5
Short circuit current [A]	6.34
Operating Cell Temp [°C]	50
Power Tolerance Range [%]	0/+3

4.2.2. Solar Panels by ENERGIASOLARE

The power rating and voltage of 24V of the panel by energiasolare falls in one of the two options of power rating discussed in previous chapter. Again, the short circuit current it has can equally be considered since it is close to the values used in the parameter estimation. Due to this, it makes it one of the best selections.

Figure 16: Panel from EnergiaSolare [24]

Figure 16 is a 24V, 250Wp solar panel produced by energiasolare. Figure 17 displays the datasheet of the panel.

Manufacturer	Energiasolare100
Shipped in	24-48h
Peso	17.8000
Potencia nominal (W)	250
Tensión V	24
Punto Máxima Tensión (Vmp)	30.5
Tensión circuito abierto (Voc)	37.7
Corriente de cortocircuito (Isc)	8.85
Corriente en el punto de máxima potencia (Imp)	8.2
Celdas	Policristallino
Dimensiones	1640x992x35
Massima Tensione Ingresso PV	30V
PF	>0.5
Eq. Watts (W)	0

Figure 17: Datasheet of the 24V,250Wp solar panel [24]

4.2.3. Solar Panels by Moscatelli

Moscatelli, a company specializing in designing, constructing, and supplying solar panels and other products for campers, vans, and mini-vans, offers a 200Wp, 12V photovoltaic panel specifically designed for those who embrace an off-grid lifestyle [25]. The image of the product is shown in Figure 18.

Figure 18: 200Wp, 12V Solar Panel [25]

The technical data of the searched product is displayed in Table 8.

Table 8: Technical Data [25]

Weight	11.5kg
Dimension	1425x705x35mm
Peak power	200Wp
Short circuit current	5.25A
Open circuit voltage	48.50V
Maximum power voltage	41.6V
Current at maximum power	4.9A
Cell efficiency	22.5%

4.2.4. Solar Panels by Solarbex

Figure 19: Panel from Solarbex

FICHA TECNICA

- Potencia (en Wattios): **250W**
- Voltaje en circuito abierto (Voc): **38V**
- Voltaje en el punto de máxima potencia (Wmp): **30,3V**
- Corriente de cortocircuito (Isc): **8,75A**
- Corriente nominal (Impp): **8,26A**
- Sistema de voltaje máximo: **1000VDC**
- Rendimiento: **15,37%**
- Tolerancia: **+/-3ºC**
- Tipo de célula: **Policristalino**
- Dimensiones: **1640 x 992 x 40 mm**
- Peso: **18,5 Kg**
- Garantía contra defectos de fabricación: 12 años

Figure 20:Technical data.

This solar panel in all standards meets the exact panel needed in this application. However, it was out of stock during the investigation. Its technical specifications are shown in Figure 20. Solarbex is known to be one of the best industries as far as panel designs are concerned.

Table 9: Solar Panel Options Compared

Available Panels	Manufacturer	Rated Voltage[V]	Voltage at Pmax[V]	Power [W]
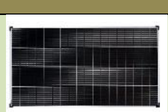	Enjoy Solar	24	36.2	200
	EnergiaSolares	24	30.5	250
	Moscatelli	12	41.6	200
	Solarbex	24	30.3	250

4.3. Available commercial Dual MPPT Solar Charger Inverter

The charger of the robot is an ac adapter while the battery storage will require dc/dc charging. Moreover, other components such as the Wi-Fi connection port and Jetson Nano also make use of ac charger hence need 230Vac/50Hz. Based on this, a solar charger inverter with a dc output is a necessity. Thus, searching for Dual solar charger inverters for this application.

It must be noticed that the system must be able to be scaled in the future, to include hybrid generation. This means that the selected inverter needs to include a specific connection for a Wind Generator or an ICE Generator, in order to cover for generation demand under no sunlight circumstances.

4.3.1. Controller By Green Cell

Figure 21: Dual MPPT Solar Inverter Charger [26]

Table 10: Specification of solar inverter by Green Cell industry [26]

Battery Voltage	24V
Dimensions	325x290x118mm
Weight	6.8kg
Output voltage	230Vac
Continuous power	3kW
Output frequency	50 or 60Hz
Max. charging current	80A
PV voltage range of MPPT	30-120Vdc
PV Power range for MPPT	1.5kW
MPPT output current	50A
Inverter efficiency	90% - 93%

This option of controller would be right for the project but lacks a communication port, which is essential in the application. Again, the power rating is far greater than the power of load to be supplied. The device's efficiency will be extremely poor when applied in this proposed model due to high power capacity. 3kW power is extremely higher than the power needed by all peripherals in the system.

4.3.2. Controller By ECGSOLAX

The EGCSolax controller has several capabilities which include integrated MPPT charge controller with voltage range of 20-150V. It charges 12V batteries including LiFePO4 batteries and lithium-ion batteries. It takes energy from solar panels and charges battery storage connected to it. The device is shown in Figure 22: 1kW, 230Vac, 12V dc solar charger Figure 22. It provides 4 charging stages, with protection against overload, over temperature and short circuits. Inclusive of its features is intelligent fans which improve battery action, decreases heating thereby extending the lifespan of the device.

Figure 22: 1kW, 230Vac, 12V dc solar charger controller.

To the advantages of this device, its power rating is enough to supply the load's consumption and power to other peripherals in the system.

4.3.3. Controller By Mile Solar

In Figure 23 is a 1kW-12kW solar inverter with MPPT charger controller [27]. As the image indicates, this inverter has dedicated features for an ICE generator which makes it a reliable and sustainable energy companion. However, these capabilities can only of use in advanced projects. Battery bank is charged using MPPT control method.

The power specifications needed by the customer from the inverter can be programmed. Assuming a 1.5kW power rating, Table 11 contains technical parameters of the solar inverter.

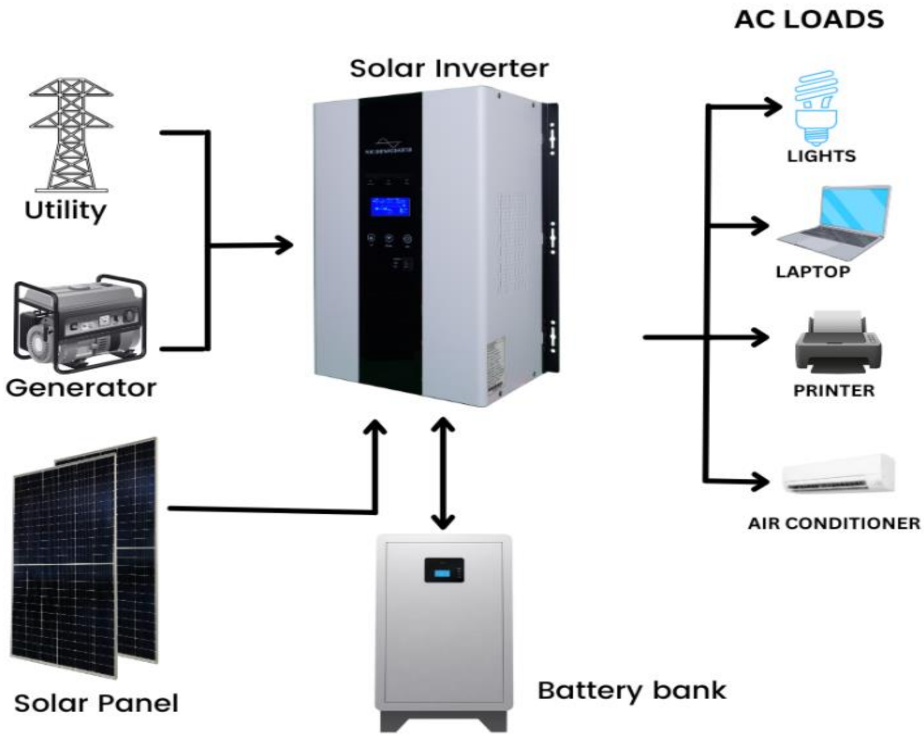

Figure 23: Solar inverter by Mile Solar which has compatibility with Solar and ICE generator. This feature of the controller makes it adaptable for future work [27].

Table 11: Table of Technical specifications of solar charger inverter from Mile Solar [27]

Technical Specifications Off-Grid solar inverter with power range from 1kW-12kW	
Model	1kW-3kW
Inverter Input/output	
Nominal output voltage	110/120VAC 220/230VAC
Output Frequency	50/60Hz ± (10RMS)
In-built AVR stabilizer	110/120VAC 220/230VAC
Waveforms	Pure sine wave output
AC input	
Voltage	110/120VAC 220/230VAC
Frequency Range	50Hz: 45 - 65Hz 60Hz: 55 - 65Hz 50Hz/60Hz(auto sensing)
Battery Bank Specifications	
Battery Type	Lithium battery, lead acid battery, gel battery,

	customized battery
Protections	Low voltage protection, Low voltage cutoff, Overvoltage alarm and overvoltage protection
AC charger	
Charging current	40A Max (Selectable from 0A, 10A, 20A, 30A, 40A)
Solar Charger	
Charger Type	MPPT
Maximum charging current	30A 40A 50A 60A 80A 100A selectable option
PV maximum input voltage	12V/24V(30A/40A): 90VDC 12/24V(50A - 100A): 130VDC 48V: (30A - 150A): 160VDC 96V(50A/60A): 180V 96V (80A - 150A): 280VDC
Maximum PV input power	48V/30A: 1620W 48V/40A: 2160W, 48V/50A: 2700W, 48V/60A:3240W 48V/80A: 4320W,
Protection	
Temperature	When temperature ≥ 85°C, inverter alarm; when temperature ≥ 90°C, inverter shutdown automatically
Overload Protection	Inverter automatically shut down if overload exceeds 110% rated power within 10 seconds.
Short circuit	automatic shutdown
Other Capabilities	
Display	LCD + LED indicator
Communication	RS232, RS485, WIFI
Operating temperature	-10°C ~ 70°C
Storage temperature	-10°C ~ 60°C

Moreover, energy consumption can be managed from a mobile app. The device's operating and storage temperature is what makes it suitable for outdoor application especially at the location of the project (with about -5°C during winter and relatively, 40°C during summer).

4.3.4. Controller By Shenzhen Giteno Technology company

This company is dedicated to research and development, design, production, and sales in uninterruptible power supplies (UPS) and other energy products including PV inverters and batteries. One solar inverter product designed by them is shown in Figure 24. This is a 3kW off-grid MPPT solar inverter [28].

Figure 24: 3kW MPPT solar inverter controller by Shenzhen company [28].

Some characteristics of this device are stated in Table 12. Based on its dual application nature, it can be considered for the future implementation of the project. On the contrary, the operating temperature might need to be assessed.

Table 12: Characteristics of the 3kW Solar charger inverter by Shenzhen

INPUTS	
Voltage	230VAC
Frequency range	50/60Hz
OUTPUTS	
AC voltage regulation (Batt. Mode)	230VAC ± 5%
Surge Power	6kVA
Efficiency	93%
Waveform	Pure Sine wave
BATTERY	
Battery Voltage	24VDC

Floating Charge voltage	27VDC
Overcharge protection	32VDC
SOLAR CHARGER & AC CHARGER	
Solar Charger Type	MPPT
Maximum PV Array Power	3kW
MPPT Range @ Operating Voltage	60-400V
Maximum PV Array Open Circuit Voltage	450VDC
Max. Input PV current	13A
Maximum Solar Charge Current	100A
Maximum AC Charge Current	80A
OPERATING ENVIRONMENT	
Humidity	5% to 95% relative humidity
Operating Temperature	-10°C to 50°C
Storage Temperature	-15°C to 60°C

Table 13: Solar Charger Controllers Options compared

Solar Controller	Type	Company	Ac Voltage [V]	Battery Voltage[V]	Power [kW]	Com. Port	Freq [Hz]
	MPPT	Green Cell	230	24	3	-----	50/60
	MPPT	ECGSolax	220/230	12	1	RJ45	50/60
	MPPT	Mile Solar	110/120 or 220/230	12/24	3	RS323, RS485, WIFI	50/60
	MPPT	Shenzhen	230	24	3	RJ45	50/60

4.4. Available commercial Solar Panels

After considering the available commercial options, the devices that complement each other are chosen with correct voltages and power ratings. Since the ECGSOLAX solar charger controller contains the right power needed for an efficient operation.

However, it can only charge battery of 12V potential. Therefore, in order to make purchasing of components easier and choose a battery that fits the operation of the controller, 12.8V, 100Ah battery energy storage produced by EGCSOLAX is equally selected for this first topology.

On the note that 12V potential is being chosen for the controller, solar panel is expected to operate at with voltage of 12V. In view of this, the 12V,200Wp solar panel from Moscatelli was decided on. In the future, controllers with ICE generator or wind energy adaptation will be the main focus. All selected components and budget for their purchase are listed in Table 14 and Table 15.

Table 14: Table of Selected components with their specific manufacturers

Selected Components	Characteristics	Manufacturer
LiFePO4 battery	12.8V, 100Ah	EGCSOLAX
Solar Charger Controller	1kW, 12Vdc, 230Vac	EGCSOLAX
Solar Panel	12V,200Wp	Moscatelli

Table 15: Budget of Project Peripherals

Items	Units	Manufacturer	Model	unit cost	Description	Nom. Power	Nominal Voltage	Size	Total Cost
1	2	Moscatelli200	HF250KA	102.52€	Solar Panels	200W	12V	1640 x992 x35	205.04€
2	1	EGCSOLAX	MIN-1K	250€	Inverter	1kW	12V		250.00€
3	2	EGCSOLAX	LB-12V 100AH	250€	LiFePO4 battery	750W	12.8V		500.00€
									Total= 955.04€

From the technical characteristics of the selected solar panel, time taken to charge the chosen BESS can be determined as:

Capacity range: 100Ah

Voltage of panel: 12V

Depth of discharge allowed: 50%

Battery percentage used = $50\%\ x\ 100Ah = 50Ah$,

If two of the 12V, 200Wp solar panel is used, battery charging time results to

$\frac{PV\_\text{max}\ \_Power}{Nominal\ voltage} = \frac{200\times 2}{12} = 33.333A$.

Time taken for PV to compensate for the 50Ah =$\frac{50}{33.333} = 1.5$ hours.

Based on the estimated value, a 400Wp panel will take about 2hours to charge a 100Ah capacity with 50% depth of discharge.

Chapter Five

5. Schematic and Architecture of Proposed Design

This chapter presents the main schematic and architectural view of the charging station proposed for the recharging of the developed autonomous robot by PXR company for remote operation of PV plant. The PV farm where the station needs to be located in seen in Figure 25. Figure 27 represents the setup of the proposed remote wireless hybrid solar charging station (WHSCS) while Figure 28 depicts the concept of the charging station.

The block diagram in Figure 26represents the proposed concept of the wireless hybrid solar charging station (WHSCS). WHSCS is a combination of two solar panels connected in parallel, Dual MPPT solar charger inverter, BESS, Nvidia Jetson Nano A206 (AI device), Transmitter/Receiver, an internet router and simplertk-2b-starter-kit (Real Time Kinematics) to supply power and monitor the charging of the robot battery.

The main purpose of WHSCS is to convert the solar power to electrical power to conduct the charging of the battery bank (BESS) in the remote area and recharge robots in the absence of solar energy or inadequate power generation due to environmental factors. To operate the wireless connection, an ac voltage of 230V at 50Hz is required hence the presence of solar charger inverter. Internet router ensures strong Wi-Fi connection within the station to avoid intermittent disconnection during robot charging. A debugging circuit is designed for indications using LED and controlled through the GPIOs of the AI device (NVidia Jetson Nano A206). The real time kinematic startup device is connected to the Jetson nano to create a tracking connection between the robot and the charging station.

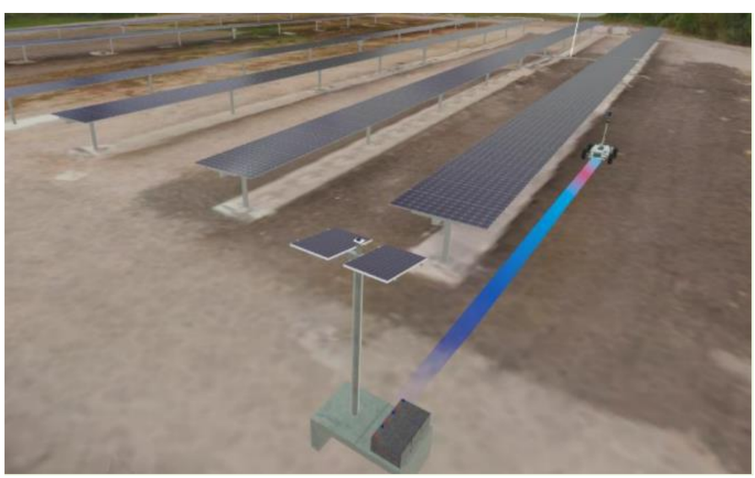

Figure 25: PV Farm where charging station is to be established [29].

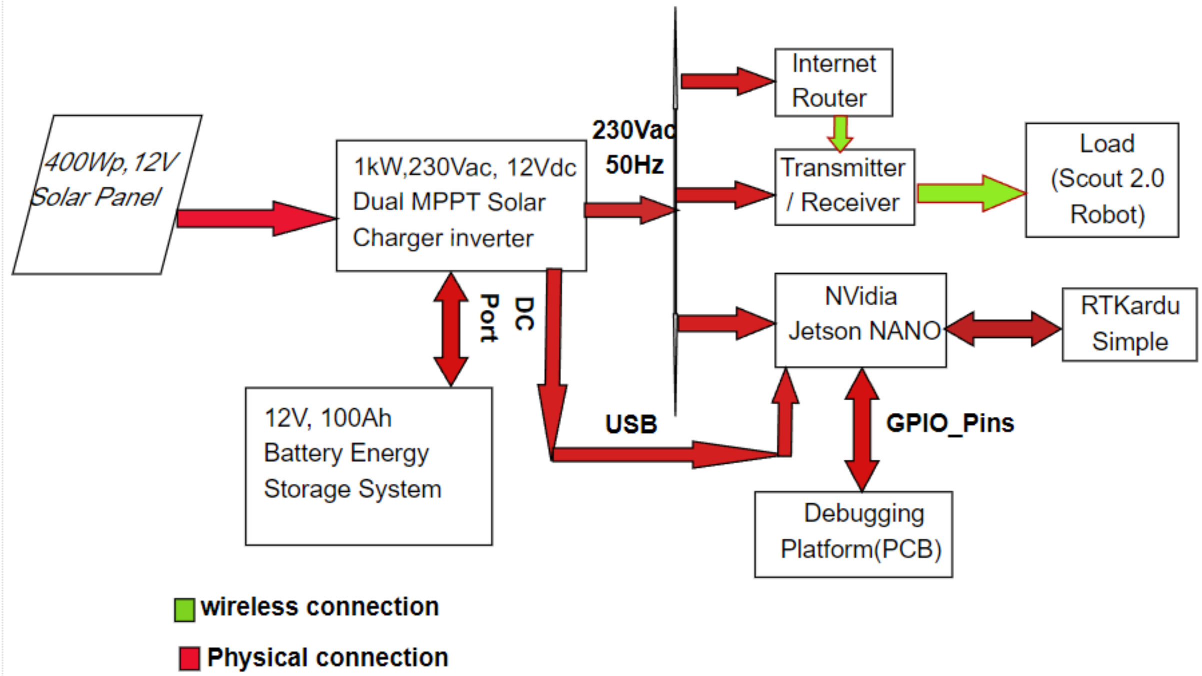

Figure 26: Block Diagram of Proposed scheme.

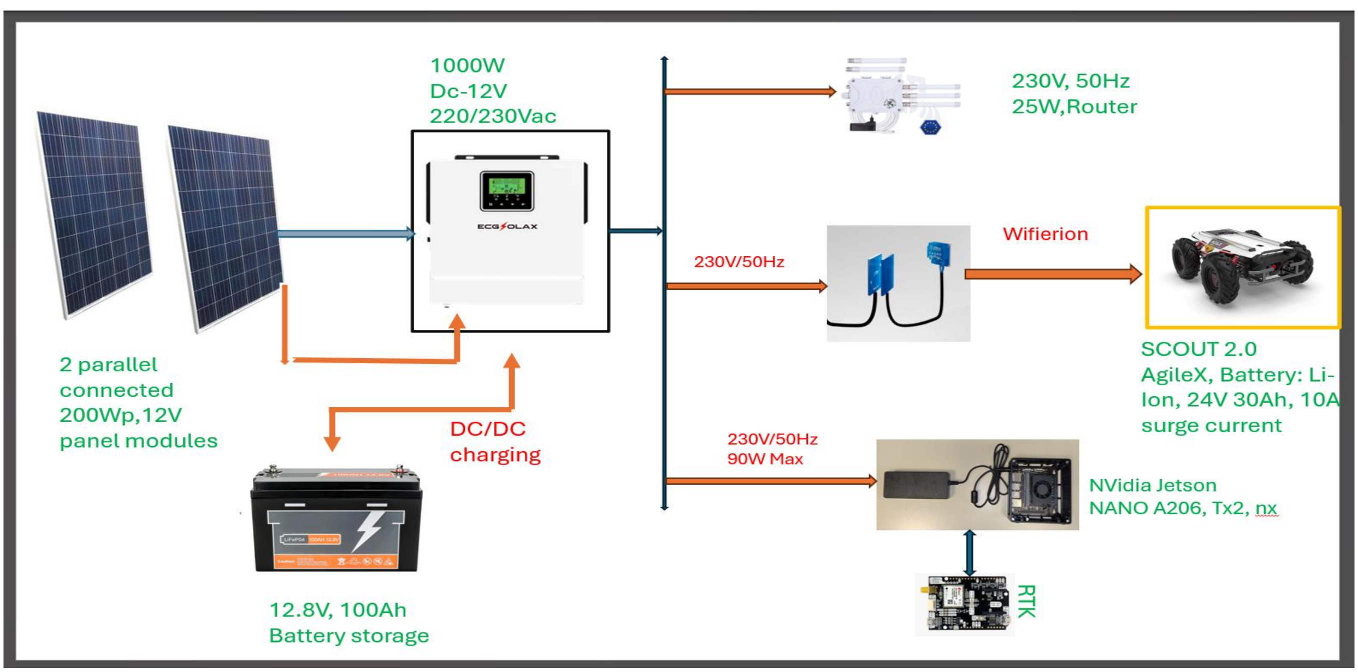

Figure 27: Wireless Charging Station Setup

In Figure 27 is illustrated the station setup. It shows the connection of the individual selected components in chapter 4. Architecture prototype of the proposed station is displayed in Figure 28. Based on the individual sizes of the necessary components, a 3D design is made using SolidWorks software. The upper pole seen in the architect is for holding the RTK and Wi-Fi for robot tracking and docking. The presence of the RTK is to operate the charging station as a real time kinematics base. It will provide a Wi-Fi relay through ubiquity to ensure connectivity with the robot in the field of operation. This will enable easy tracking of the station by the intelligent robot.

Panels are tilted towards the south at a specific angle due to the winter which depends on the position of Spain on the world hemisphere. The size of the station depends on the size of the panel used while the size of the robot determines the measurements used for the rail used to lift it from the ground into the station.

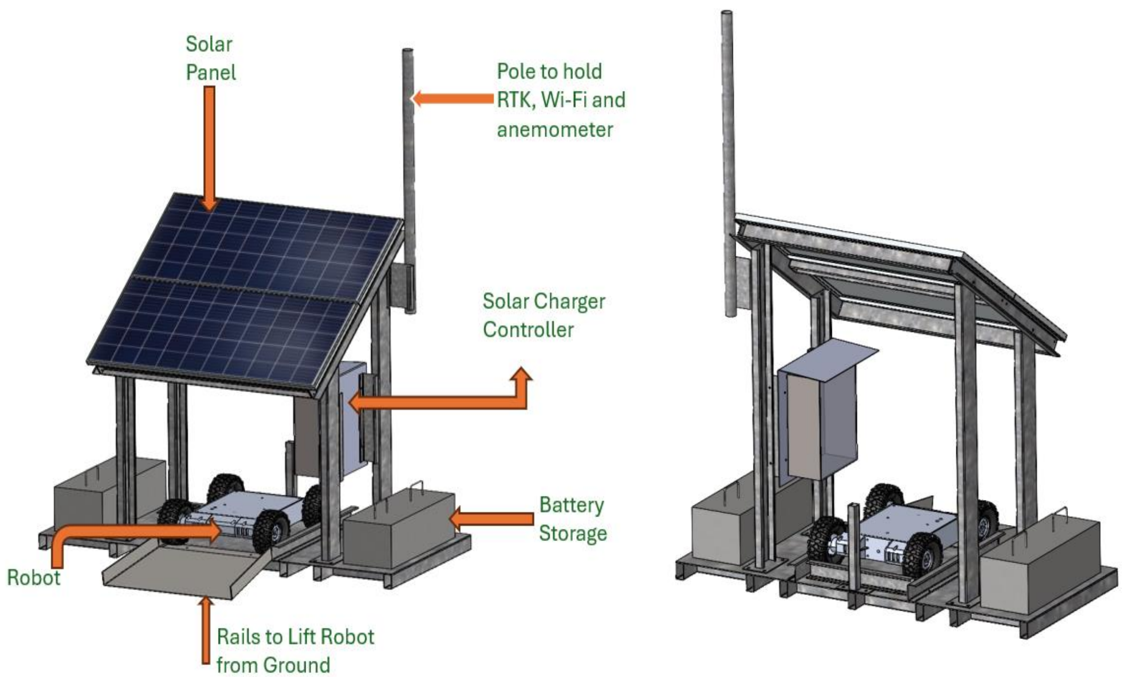

Figure 28: Prototype of Charging Station Concept [29]

The rails are incorporated in the station to lift the robot from the ground into the station. The channel in which the Robot is positioned is ensured to be fixed to assume a stable connection between controller and robot. This will avoid continuous disconnection and connection during charging.

Chapter Six

6. Development and Control of Debugging Platform

This section focuses on the design of indication lights which are controlled by the GPIOs of the Nvidia Jetson Nano. Circuits used to switch the light emitting diodes (LEDs) as well as push buttons are analysed and built using Altium designer.

6.1.PCB Design

Printed circuit board (PCB) is designed for LED switching and pushbutton regulation circuit. The LEDs and the pushbuttons are controlled with GPIO pins of the Jetson Nano through current limiting resistors and transistors. The subsections explain the component value selection and the correct circuits for this implementation.

The major purpose of the LEDs in the system is for indications during charging and connections. In the case of good contact between robot and station, the LED red must be on. After a fully charged robot, the light green must turn on. During situations where contacts with station is not stable, the yellow LED or orange can be programmed to give this awareness. The implementation of push buttons in here can be applied for trouble shooting. All these operations will require the Nano device to receive data from the robot battery as well as the charger controller and the battery charger in the system.

6.1.1. Components Required

6.1.1.1. LED Switching Circuit

Calculations done to determine the value of resistors required for LED and pushbutton circuit are outlined in this subsection. Comparing the Jetson Nano to Raspberry Pi (RPi), Nvidia Jetson Nano pins carry much less current. Thus, it is not possible to light LED directly with GPIO pins of the Nano hence a switching transistor is the solution to this problem. Current limiting resistors, P2N2222ATA transistor and 5V supply are required.

In order to reduce the amount of current drawn by the LED, a current limiting resistor is used at the cathode. In order to choose the correct value of resistor, the forward voltage (the minimum voltage difference between the cathode and anode) that needs to be supplied to the Led must be known. Forward current which is the maximum current the LED can manage continuously. Table 16 contains the datasheet of the LED to be used in the circuit.

Table 16:Datasheet of available LED (ELM12755GD)

Parameter	Value
Forward Voltage[V]	2.1
Forward Current [A]	30m

The LED used as indicated in Table 16 has a forward voltage of 2.1 and current of 30mA. 5V voltage is supplied from the Jetson Nano 5V pin to drive the LED. In this case, using the ohms law, resistance value is estimated as follows.

$$R = \frac{\Delta V}{I} = \frac{(5 - 2.1)}{0.030A} = 96.7\Omega$$

However, resistors do not usually appear in 96.7Ω. Moreover, in built tolerances can cause variances from the actual resistance. Using this resistance value will still cause the LED to run at maximum current hence in order to drastically reduce the current, resistance of 330Ω is used instead of the calculated one. By using 330Ω, the current through the LED is limited to 8.8mA.

As stated earlier, the transistor will function as a switch to provide enough current to turn on the LED since the Jetson Nano GPIO pin does not have the capability to power the LED alone. The purpose of the transistor is to amplify power. An NPN bipolar junction transistor (BJT) is used in this low power switching circuit. The P2N2222ATA transistor is controlled by signal from jetson Nano through its base while the emitter is grounded, and power is supplied to the collector. In addition, an open circuit occurs between collector and emitter of the transistor when Jetson GPIO pulse is low (Transistor on Cutoff mode). Applied current at the transistor base causes it to saturate, creating a short circuit between collector and emitter. Current then flows turning the LED light up. Figure 29 depicts the schematic of the LED circuit used.

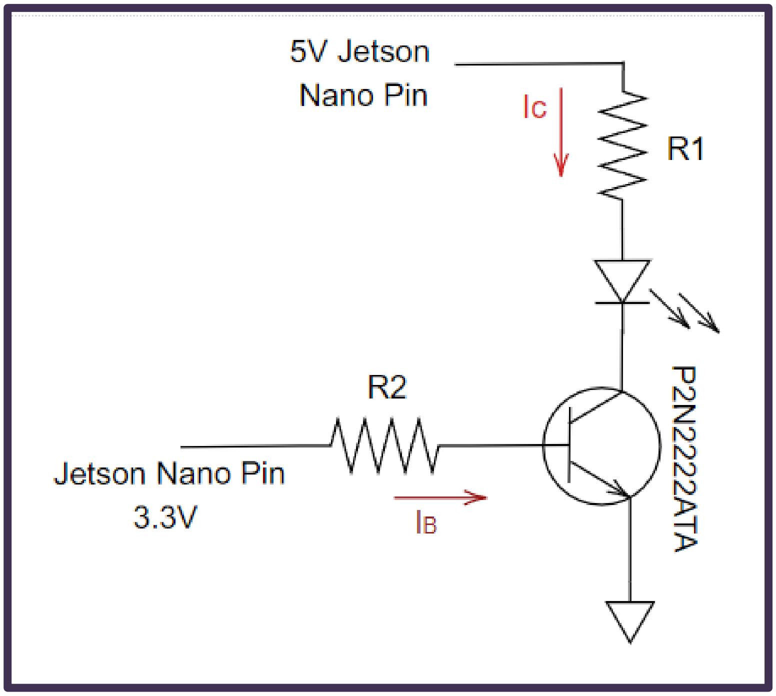

Figure 29: LED Switching Circuit

R2 is the base resistor which determines the base current of the transistor. This resistor performs the same function as the current limiting resistor on the LED. Since the collector current drawn by the LED is 30mA, base current can be estimated as:

$$I_B = \frac{I_c}{h_{fe}} = \frac{0.03}{100} = 0.0003A$$

Where h_{fe} is the dc gain of the transistor. Using voltage drop between collector and emitter (for this transistor is 0.7V). Potential in the GPIO pins is 3.3V. With these values the transistor base resistance can be calculated as:

$$R_2 = \frac{3.3 - 0.7}{0.0003} = 8666.7\Omega$$

Since there exist no resistor of such value of resistance, a 10k Ω resistor is chosen. Hence R_2 is selected as 10kΩ.

6.1.1.2. Pushbutton Circuit

The debugging platform includes pushbuttons which are used to regulate the pulses at the input pin connected to the base of the LED switch. Pull up resistor is used to limit current through the switch as indicated in Figure 30. Again, the use of the pull up resistor is to ensure a high state (1) on the input pin when the button is unpressed. Without it, the input floats and the input vary randomly.

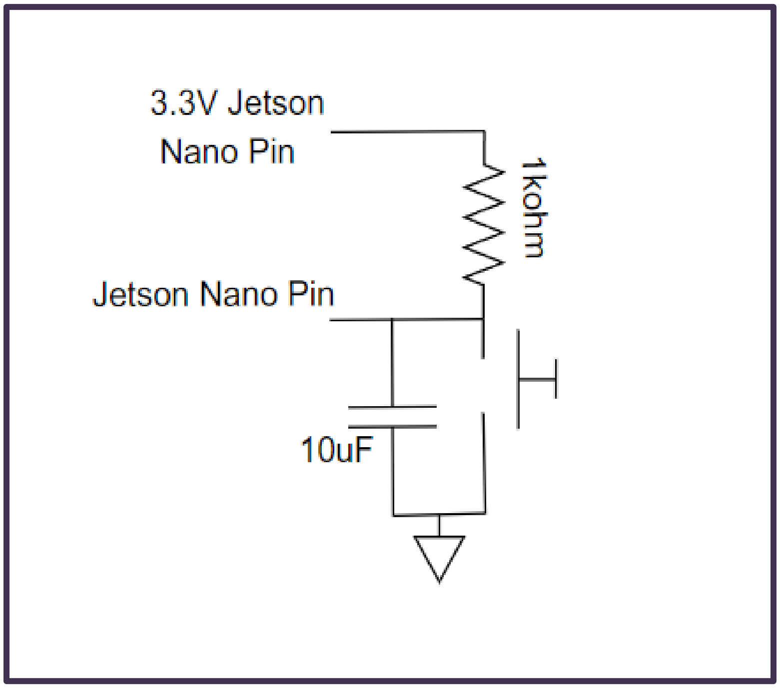

Figure 30: Pushbutton Circuit with 1kΩ Pullup Resistor.

The 10µF capacitor is to ensure constant voltage across the pushbutton and for decoupling. Both pushbutton and LED circuits are designed on a circuit board using Altium designer.

6.1.2. PCB Design in Altium

The circuit board is designed with four LEDs (Red, Yellow, Green, and Blue) and four pushbuttons. Each push button will be used to control each LED. These colors of LEDs are to be used as indicators for fully charged battery, not connected and others. The Schematic of the PCB design is presented in Figure 31. Figure 32 and Figure 33 are the top and bottom layer of the circuit board designed respectively. In Figure 34 is the layout of the PCB in Altium.

Budget of the components used for the PCB design is noted down in Table 17.

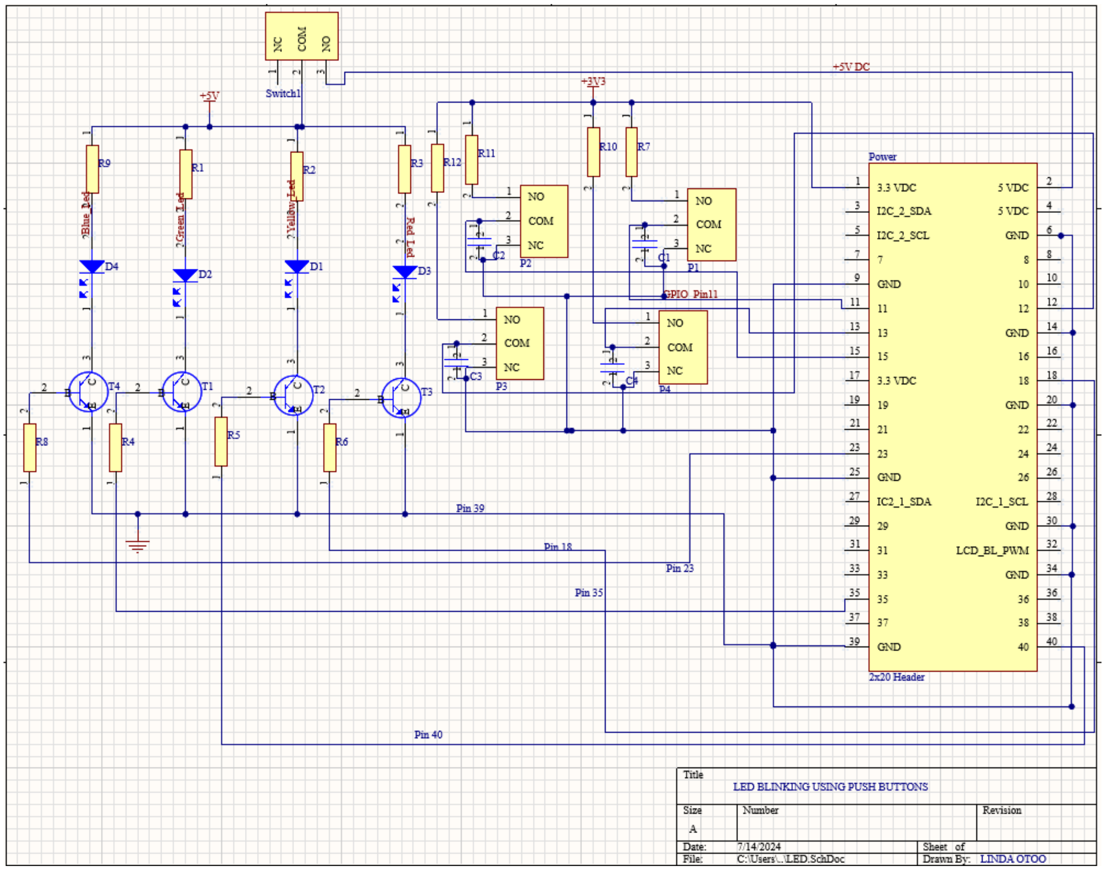

Figure 31: Schematic of PCB

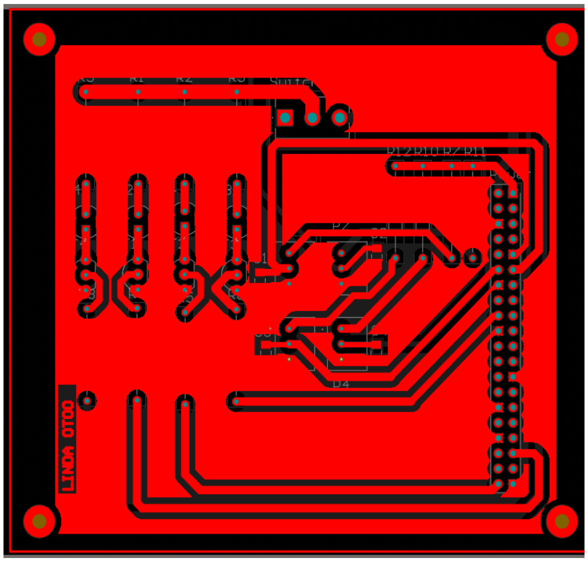

Figure 32:PCB Top Layer view

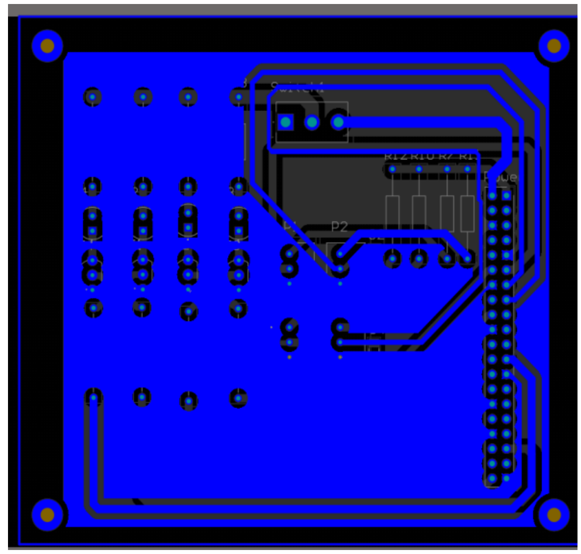

Figure 33: PCB Bottom Layer view

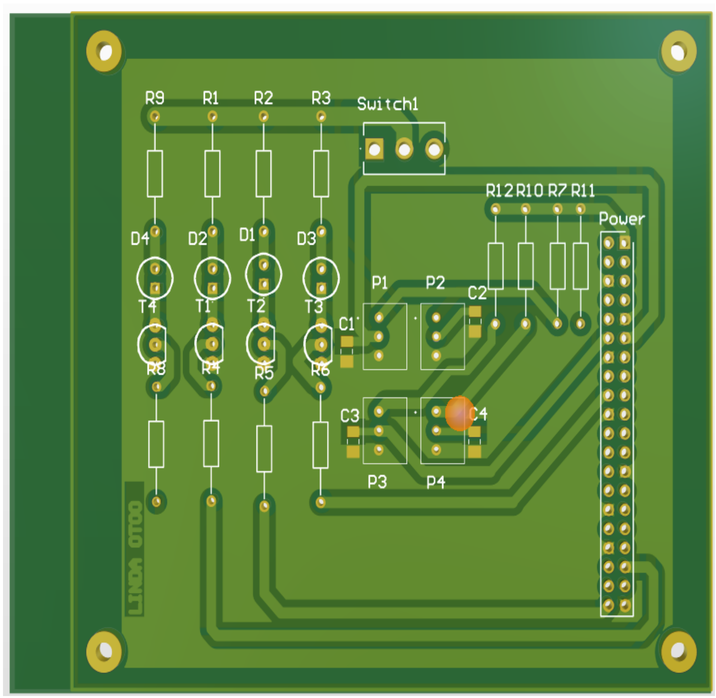

Figure 34: PCB Layout (3D view)

Table 17:Budget for PCB Design

	Component description	Reference in RS	Manufacturer's reference	Price / unit (€)	Quantity	Total Price
1	onsemi PN2222ATA	739-0381	Onsemi: PN2222ATA	0.249	4	1.00 €

	NPN Transistor, 1 A, 40 V, 3-Pin TO-92					
2	MLCC SMD 1206 25V 10uF X7R 10% T: 1.6mm	242-7420	TDK: C3216X7R1E106K160AB	0.498	4	1.99 €
3	Pulsadores	633-BB15AP	NKK Switches: BB15AP	3.93	4	15.72 €
4	Alojamientos de cables y cabecera 20+20 DIL VERTICAL PIN HEADER GOLD+TIN	855-M20-9762042	Harwin: M20-9762042	1.46	1	1.46 €
5	Cables planos / cables IDC Slim Body Double-Row IDC Socket Assemblies, 0.100" Pitch	200-IDSD20D0320G	Samtec: IDSD-20-D-03.20-G	12.94	1	12.94 €
6	Led Verde	749-ELM12755GD	Bivar: ELM12755GD	0.68	1	0.68 €
7	Led Amarillo	749-ELM70303YD	Bivar: ELM70303YD	0.5	1	0.50 €
8	Led Azul	749-ELM13705BWD	Bivar: ELM13705BWD	1.24	1	1.24 €
9	Led Rojo	2508429109	Lumex: SSL - LX30521D	0.06728	1	0.06728
10	Switch	448-0747	RS-PRO: 448-0747	2.225	1	2.225
11	1kOhm resistencia	739-7459	MULTICOMP PRO: MCF 0.25W 1K	0.85	4	3.4
12	10kohm resistencia	739-7538	MULTICOMP PRO: MCF 0.25W 10K	0.85	4	3.4
13	330ohm resistencia	707-7622	RS PRO: 707-7622	0.123	4	0.492
						TOTAL
						45.11 €

The purchase of all relevant components used for this circuit board amounts to 45.11€.

6.2. Programming of Nvidia Jetson Nano

Figure 35 displays the developer kit of Jetson Nano by Nvidia. The parts of the device are carefully indicated and described.

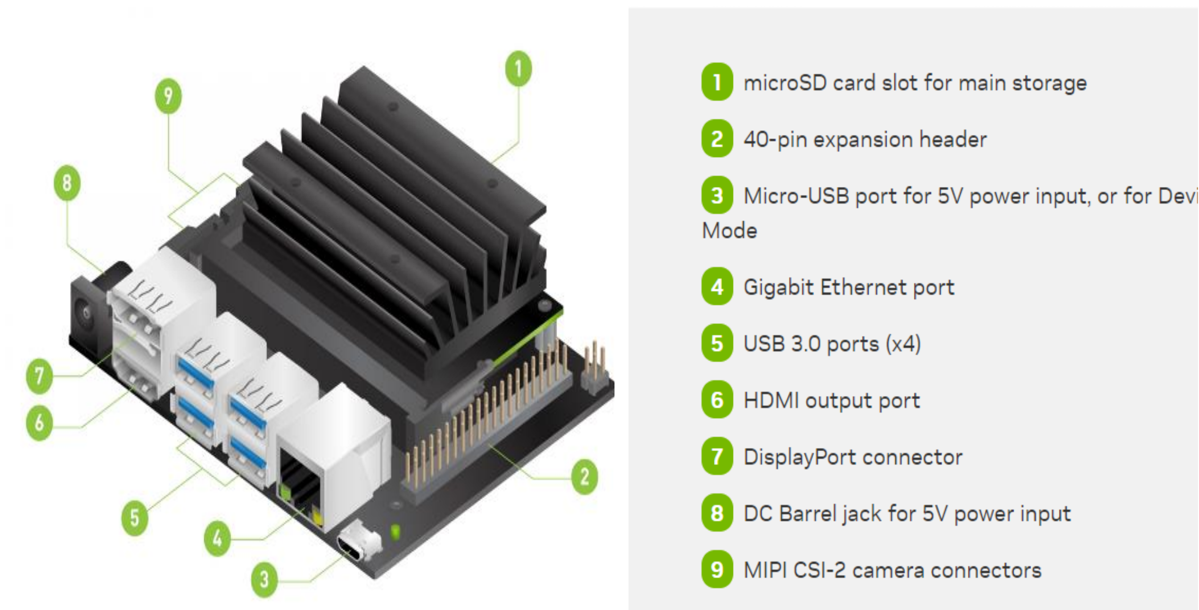

Figure 35: Nvidia Jetson Nano Developer Kit [30]

The Nvidia Jetson Nano developer Kit is defined as a small AI computer used for cool AI robot applications and more [30]. It contains forty-one (41) header pins with forty GPIOs. Below Figure 36 which contains information that describes each GPIO pin of the Jetson Nano device.

SoC GPIO	Linux GPIO #	Alternate Function	Default Function			Default Function	Alternate Function	Linux GPIO #	SoC GPIO
			3.3 VDC	1	2	5 VDC			
PJ.03	75	GPIO	I2C1_SDA	3	4	5 VDC			
PJ.02	74	GPIO	I2C1_SCL	5	6	GND			
PBB.00	216	AUD_CLK	GPIO	7	8	UART1_TXD	GPIO	48	PG.00
			GND	9	10	UART1_RXD	GPIO	49	PG.01
PG.02	50	UART1_RTS	GPIO	11	12	GPIO	I2S0_SCLK	79	PJ.07
PB.06	14	SPI1_SCK	GPIO	13	14	GND			
PY.02	194		GPIO	15	16	GPIO	SPI1_CS1	232	PDD.00
			3.3 VDC	17	18	GPIO	SPI1_CS0	15	PB.07
PC.00	16	SPI0_MOSI	GPIO	19	20	GND			
PC.01	17	SPI0_MISO	GPIO	21	22	GPIO	SPI1_MISO	13	PB.05
PC.02	18	SPI0_SCK	GPIO	23	24	GPIO	SPI0_CS0	19	PC.03
			GND	25	26	GPIO	SPI0_CS1	20	PC.04
PB.05	13	GPIO	I2C0_SDA	27	28	I2C0_CLK	GPIO	18	PC.02
PS.05	149	CAM_MCLK	GPIO	29	30	GND			
PZ.00	200	CAM_MCLK	GPIO	31	32	GPIO	PWM	168	PV.00
PE.06	38	PWM	GPIO	33	34	GND			
PJ.04	76	I2S0_FS	GPIO	35	36	GPIO	UART1_CTS	51	PG.03
PB.04	12	SPI1_MOSI	GPIO	37	38	GPIO	I2S0_DIN	77	PJ.05
			GND	39	40	GPIO	I2S0_DOUT	78	PJ.06

Figure 36: GPIO Pin Labels and Numbers.

Chapter Seven

7. Experiment and Result

This chapter presents the experiments performed on the PCB design. Before the PCB configuration, tests were done with the estimated values of resistance, selected LEDs, pushbutton and transistor.

7.1. Test Before PCB Design

During the experiment a breadboard, Nvidia Jetson Nano GPIO, P2N2222ATA transistor, pushbutton and a red LED. Jetson Nano was programmed in python language to regulate the push button which directly controls the base pulse of the transistor. This first test was done for only one LED since the circuit will be same for all the LEDs. Figure 37 is a display of the setup made with the bread board for the experiment while the Figure 38 consist of the code implementation for the test Kit.

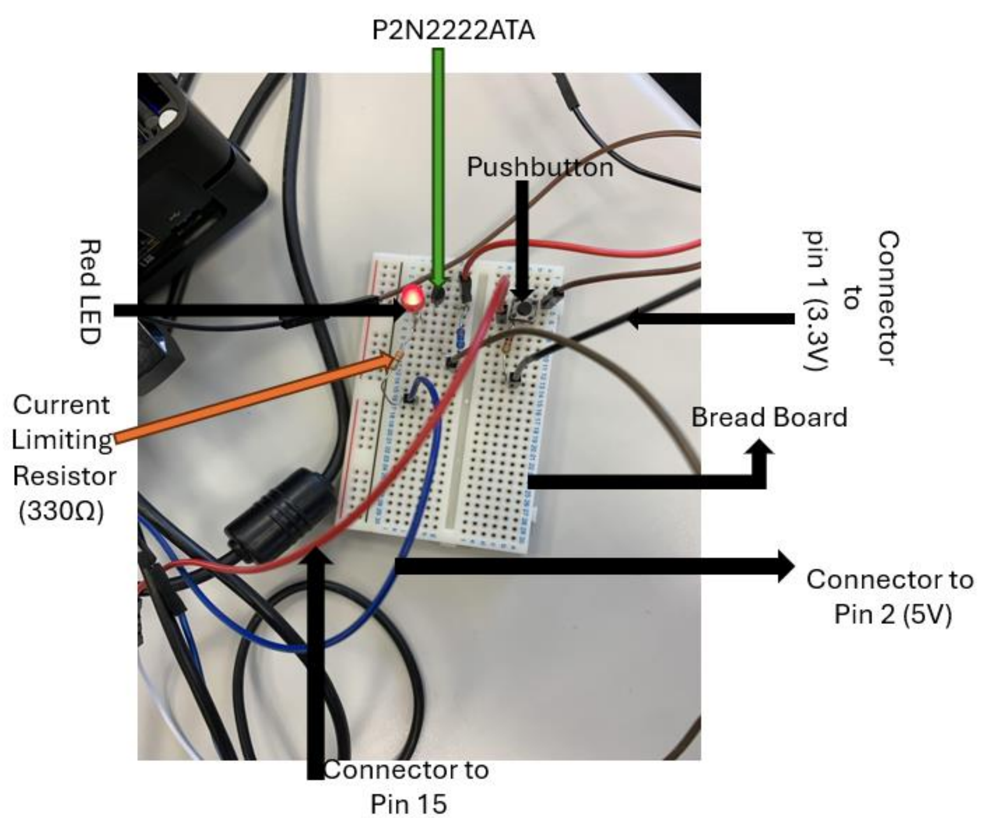

Figure 37: Test Board with connections of the necessary components.

```
import RPi.GPIO as GPIO
import time
GPIO.setmode(GPIO.BOARD) #Set mode for the GPIOs
inpin =  15  #Indicate input pin number
outpin = 13  #Indicate input pin number
Ledstate=0   #Setting initial state of LED(on/off)
PbuttonstateOld=1    # Setting the state of the pushbutton(True(1)/False(0))
GPIO.setup(inpin,GPIO.IN) #Set GPIO as input
GPIO.setup(outpin,GPIO.OUT) #Set GPIO as output

#Loop of operation. Controlling the LED with pushbutton state
while (1==1):
    PbuttonstateNew=GPIO.input(inpin)
    if PbuttonstateOld==0 and PbuttonstateNew==1:
      Ledstate=not(Ledstate)
    GPIO.output(outpin,Ledstate)
    x=PbuttonstateNew   #Reading the input of the model(Pushbutton)
    print(x)
    PbuttonstateOld=PbuttonstateNew  # Update state of pushbutton
```

Figure 38: Code Implemented to switch LED by controlling the pushbutton through GPIO pins 13 and 15, respectively.

The GPIO pin thirteen is set as an output since it is used to control the turn on or off of the LED. Depending on whether the push button is pressed or not, pin thirteen (13) can be high or low. Considering this, push button becomes the input to the system. Therefore, the if condition used is to control the state of the LED when the push button is pressed or released.

7.2. Experiment Done Using PCB and Jetson Nano

Since the first test done with the bread board was successful, the PCB was designed, soldered and assembled. Figure 39 shows the assembled PCB.

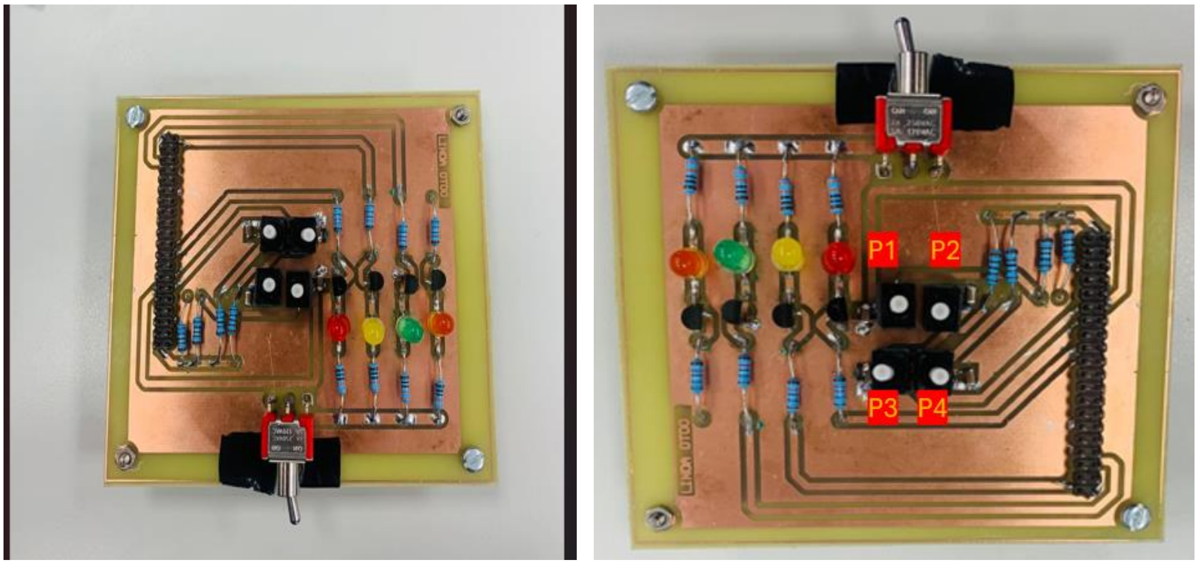

Figure 39: Assembled PCB

The switch seen on the board is to control the power supply to the LEDs. The complete setup for the experiment and testing of the code and PCB is illustrated in Figure 40.

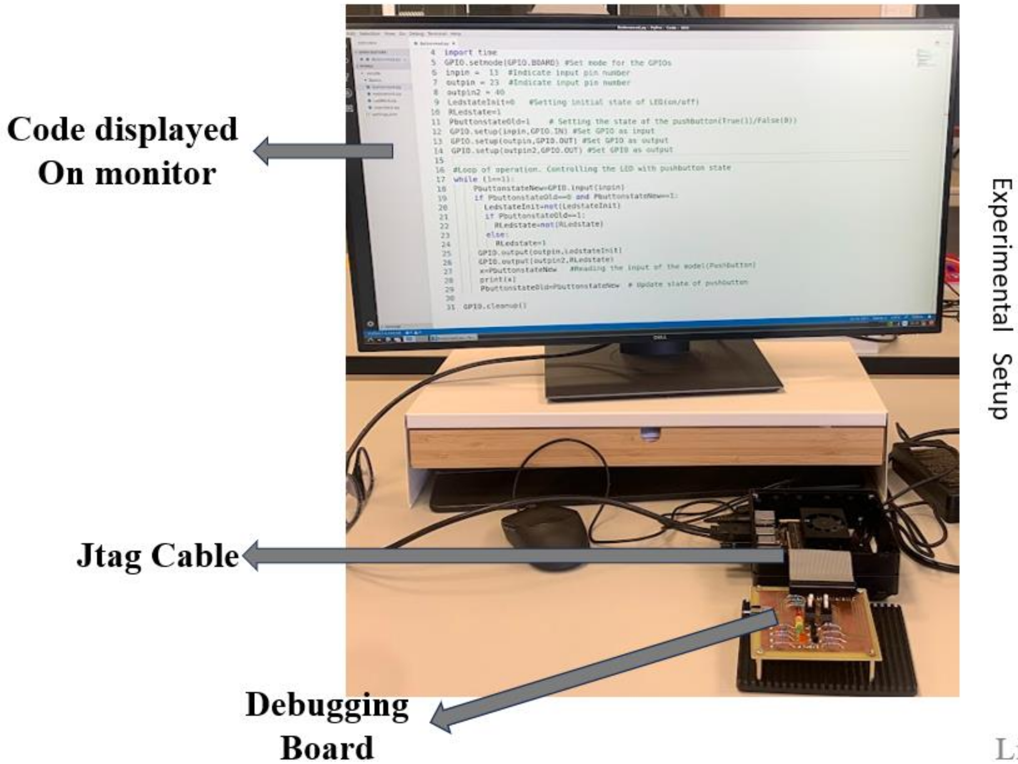

Figure 40: Experimental Setup

The Jtag cable aids in the direct connection of the Jetson Nano Pins to the circuit board as indicated in Figure 41. Using the python programming language, a code is written to light up the LED when any of the pushbuttons is pressed. The pushbutton to be pressed depends on which one has been programmed as an input.

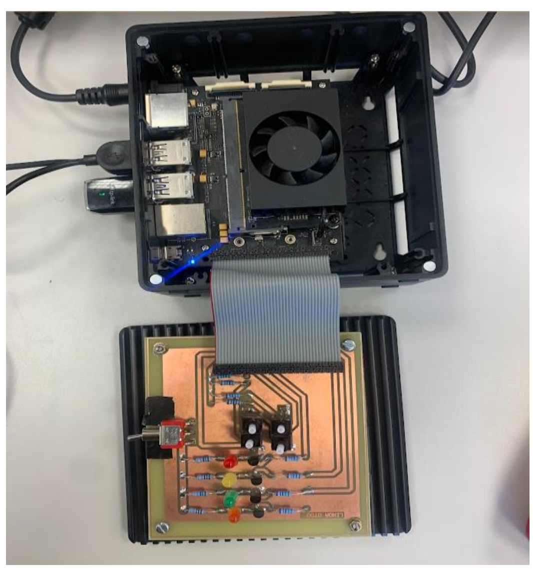

Figure 41: Nvidia Jetson Nano connected to PCB board using Jtag Cable.

In the test done, all the four LEDs were regulated by pushbutton 1 which corresponds to pin 11 on the Jetson Nano. Therefore, pin 11 is set as an input to the system. All four LEDs are set as outputs when the input from the pushbutton is applied. GPIO pins used for each of the LEDs and Pushbuttons are stated in Table 18.

Table 18: Table of GPIO Pins Set for the LEDs and Pushbuttons and Power supply to the Board by the Jetson Nano

Component	GPIO Pins (Set Mode: BOARD)
Pushbutton 1	11
Pushbutton 2	15
Pushbutton 3	12
Pushbutton 4	13
Red LED	18
Yellow LED	40
Green LED	35
Orange LED	23
Ground	39/6
5V supply to LEDs	2
3.3V supply to Pushbuttons	1

```
import os
os.environ['JETSON_PLATFORM'] = 'JETSON_XAVIER'
import RPi.GPIO as GPIO
import time
GPIO.setmode(GPIO.BOARD) #Set mode for the GPIOs
inpin =  11  #Indicate input pin number for pushbutton 1
outpin = 23  #Indicate outpin pin number for Orange LED
outpin2 = 40 #Indicate outpin pin number for Yellow LED
outpin3 =  18 #Indicate outpin pin number for Red LED
outpin4 = 35 #Indicate outpin pin number for Green LED
LedstateInit=0   #Setting initial state of Orange LED(on/off)
RLedstate=0   #Setting initial state of Red LED(on/off)
YLedstate=0 #Setting initial state of Yellow LED(on/off)
GLedstate=0 #Setting initial state of Green LED(on/off)
PbuttonstateOld=1    # Setting the state of the pushbutton(True(1)/False(0))
GPIO.setup(inpin,GPIO.IN) #Set GPIO as input
GPIO.setup(outpin,GPIO.OUT) #Set GPIO as output
GPIO.setup(outpin2,GPIO.OUT) #Set GPIO as output
GPIO.setup(outpin3,GPIO.OUT) #Set GPIO as output
GPIO.setup(outpin4,GPIO.OUT) #Set GPIO as output

#Loop of operation. Controlling the LED with pushbutton state
while (1==1):
    PbuttonstateNew=GPIO.input(inpin)
    if PbuttonstateOld==0 and PbuttonstateNew==1: # Setting Condition
      LedstateInit=not(LedstateInit)
      RLedstate=not(RLedstate)
      YLedstate=not(YLedstate)
      GLedstate=not(GLedstate)
    GPIO.output(outpin,LedstateInit)
    GPIO.output(outpin2,YLedstate)
    GPIO.output(outpin3,RLedstate)
    GPIO.output(outpin4,GLedstate)
    x=PbuttonstateNew   #Reading the input of the model(Pushbutton)
    print(x)     # Printout Results
    PbuttonstateOld=PbuttonstateNew  # Update state of pushbutton
```

Figure 42: Program written to toggle Led based on state of push button

The code viewed in Figure 42 is used to regulate the turning on and off of all four LEDs using the pushbutton 1. The result of this experiment is displayed in Figure 43 to Figure 45.

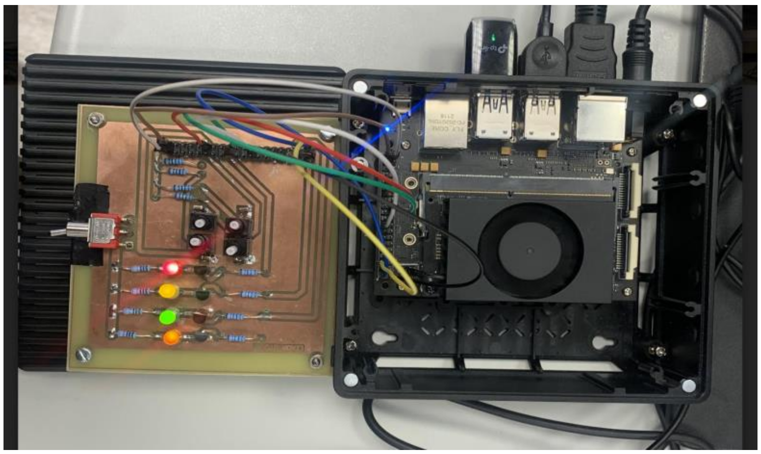

Figure 43: All LEDs on

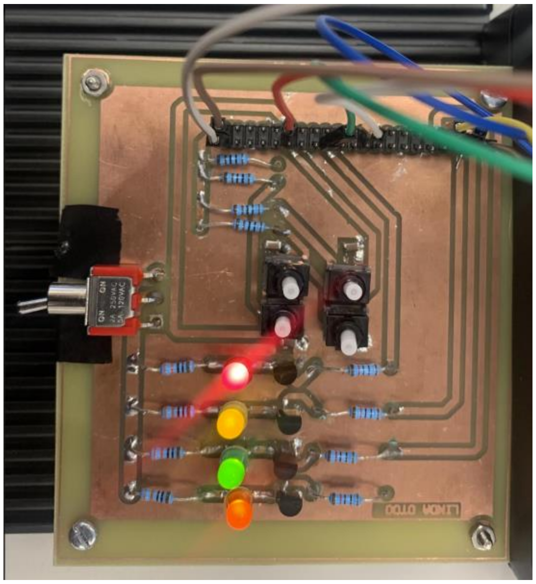

Figure 44: Clear View of all LEDs on

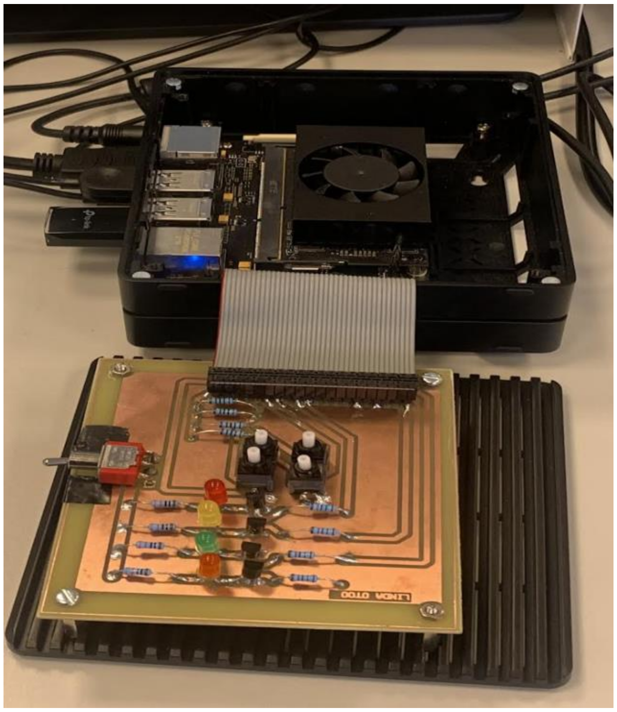

Figure 45: All LEDs turn off

This operation of turning on and off of LEDs is done in a loop. Thus, depending on the state of the LED as it is pressed, the outputs seen at the GPIO pins set as output could be 1 or 0 (True or False respectively). If it is 1, the LED turns on else, Led turns off.

Chapter Eight

8. Conclusions and Outlook

This chapter presents the main conclusions reached out of the work and puts light on the main covered issues and the present work situation. Then an outlook is proposed for the future work.

8.1. Conclusions

Short paragraph indicating a summary of the conclusions.

The following points are the main aspects that have been studied and conclusions reached in each.

- The size of battery energy storage capacity depends on the capacity of the load to be supplied if solar panel power is fixed. Moreover, the time taken to charge a battery to its full capacity is based on the energy used and the depth of discharge. The higher the depth of discharge the longer it takes to charge. Again, the time depends on the current of the solar panel used.

- The components selected for a prototype must be available commercially with several options since the design of the system might change. Budget is made to know the cost of the project to be done for accountability and easy analysis especially if the product is to be produced and sold.

- A Nvidia Jetson Nano A206 developer kit has been implemented for control and communication between robots and other peripherals in the charging station during docking. The Nano is programmed to light LED by regulating pushbuttons. Specific circuits required for this platform are investigated in detail due to lower current in its GPIO pins compared to Raspberry Pi pins.

- The printed circuit board of LEDs and pushbuttons debugging platform has been designed, soldered and assembled Using Altium designer.

- As a final step, experimental test has been conducted on the PCB using the Nvidia Jetson Nano developer kit

8.2.Future Work

Specific to the topic under study, many issues show motivations for study and implementation, among these issues are the following:

- Building an ADC conversion Board for the Nvidia Jetson Nano since it does not have an in-built analogue digital conversion. Using the ADC conversion, the LEDs operation can be based on the charging level of the Robot battery. Also contact between transmitter and receiver, hence communication between them and the Nano must be established.

- Selection of correct size of Cabinet to contain all components

- Assembling of all components for the charging station. This includes solar panels, solar inverter charger, router, battery energy storage, anemometer, Jetson Nano, PCB and the RTKsimple developer kit.

- Advanced design considering hybrid charging station with wind generator or ICE generator. The topology describing this improved version is shown in Figure 46.

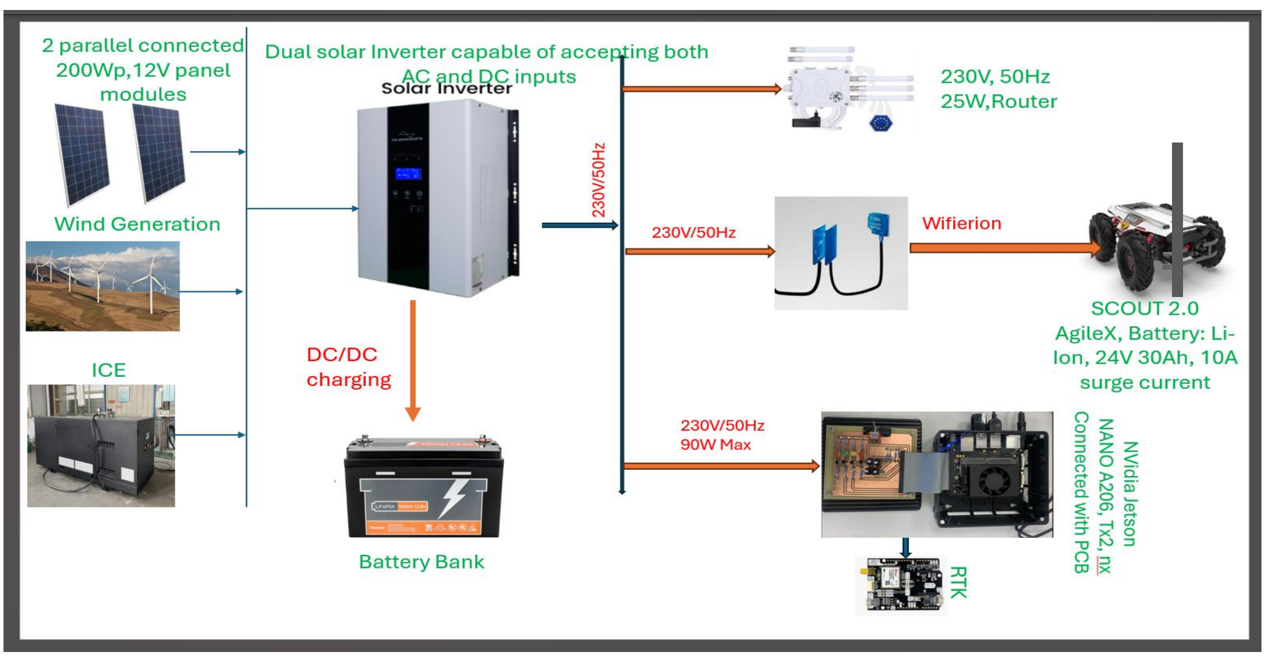

Figure 46: Future Topology of Wireless charging station

References

[1] R. R. a. A. P. K. R, "Sine Wave Inverter with Three Stage Battery Charger for Solar Photovoltaic Application," in *2021 IEEE Madras Section Conference (MASCON)*, 2021.

[2] D. Andre, "allaboutai," allaboutai, 4 December 2023. [Online]. Available: https://www.allaboutai.com/ai-glossary/autonomous-robot/. [Accessed 7 July 2024].

[3] K. S. C. a. G. K. Nisha, "Review of Autonomous Mobile Robots," in *2024 International Conference on E-mobility, Power Control and Smart Systems (ICEMPS)*, Thiruvananthapuram, India, 2024.

[4] S. Nitin, P. Jitendra Kumar and M. Surajit, "A Review of Mobile Robots: Applications and Future Prospect," *International Journal of Precision Engineering and Manufacturing,* vol. 24, no. 20/08/2023, p. 12, 2023.

[5] D. M. &. C. G. D. Considine, "Robot technology fundamentals," in *Standard handbook of industrial automation*, Springer, 1985, pp. pp. 262-320.

[6] D. Nitzan, "Development of intelligent robots: Achievements," *IEEE Journal on Robotics and Automation,,* vol. 1, p. 13, 1985.

[7] N. N. K. a. A. A. G. V. A. Sansare, "Design of Standalone PV Charging System for Lead Acid Battery using Controlled Boost Converter,," in *International Conference on Current Trends in Computer, Electrical, Electronics and Communication (CTCEEC)*, Mysore, India, 2017.

[8] S. B. B. S. W. H. M. N. M. K. a. A. R. I. S. Naik, "Design and Performance Analysis of Standalone Solar PV based Electric Vehicle Charging Station," in *Karnataka Subsection Flagship International Conference (NKCon),*, Belagavi, India, 2023.

[9] A. V. a. B. Singh, ""A Solar PV, BES, Grid and DG Set Based Hybrid Charging Station for Uninterruptible Charging at Minimized Charging Cost," in *IEEE Industry Applications Society Annual Meeting (IAS)*, Portland, OR, USA, 2018.

[10] E. H. C. Harik, "Design and Implementation of an Autonomous Charging Station for Agricultural Electrical Vehicles," *Applied Sciences,* vol. 11, 2021.

[11] P.Manimekalai, R.Harikumar and S.Raghavan, "An Overview of Batteries for Photovoltaic (PV) Systems," *International Journal of Computer Applications,* p. 6, 2013.

[12] V. V.-G. a. A. H. a. N. N. a. L. R.-E. a. P. Bauer, "Selecting a suitable battery technology for the photovoltaic battery integrated module," *Journal of Power Sources,* vol. 438, no. 0378-7753,

p. 227011, 2019.

[13] M. F. a. T. P. a. S. Sirtoli, "Chemical and electrochemical recycling of the negative electrodes from spent Ni–Cd batteries," *Journal of Power Sources,* vol. 163, no. 0378-7753, pp. 1114-1119, 2007.

[14] F. M. C. Nogueira, "Chemical and physical characterization of electrode," *Waste Management,* vol. 27, no. 0956-053X, pp. 1570-1579, 2007.

[15] C. Z. C. Z. Y. L. X. Hu, "Technological developments in batteries: a survey of princiipal role, types and management needs," in *IEEE Power Energy Mag*, 2017.

[16] M. M. J. S. N. O. L. V. J. V. M. G. Berckmans, "Cost projection of state of the art lithium-ion batteries for electric vehicles up to," in *Energies*, doi:10.3390/en10091314..

[17] F. W. J. L. G. Y. N. Nitta, "Li-ion battery materials: present and future,," *Today,* vol. 5, pp. 252-264, 2015.

[18] M. K. a. P. B. N. Kar, "Design and Analysis of MPPT Charge Controller," in *2021 International Conference on Simulation, Automation & Smart Manufacturing (SASM)*, Mathura, India, 2021.

[19] K. Sachin, P. K. Sharma, L. Solanki, V. P. Yadav and A. N. Mukesh, "Design and Development of PWM based Solar Hybrid Charge Controller," in *2021 IEEE International Conference on Electronics, Computing and Communication Technologies (CONECCT)*, Bangalore, India, 2021.

[20] P. Sudwilai, "A Design and Development of P I Controlled Based MPPT for Photovoltaic Systems," in *International Conference on Electrical Machines and Systems (ICEMS)*, Jeju, Korea(South), 2018.

[21] M. Company, "MANLY," Manlybattery, [Online]. Available: https://manlybattery.com/product-item/24v-120ah-lifepo4-battery/#tab-id-1. [Accessed May 2024].

[22] KepWorth, KepWorth, [Online]. Available: https://www.kepworth.com/product/12v-100ah-120ah-lifepo4-storage-battery-built-in-bluetooth-bms/. [Accessed 05 2024].

[23] Kepworth, KepWorth, [Online]. Available: https://www.kepworth.com/product/24v-100ah-rechargeable-18650-lithium-battery-with-led-lightfor-led-lamp-electric-vehicle-solar-storage-battery25-2v-charger/. [Accessed 05 2024].

[24] "ENERGIASOLARE," ENERGIASOLARE, [Online]. Available: https://www.energiasolare100.com/es/panel-solar-fotovoltaico-250w-24v-policristalino-

placa-solar.html. [Accessed 05 2024].

[25] Moscatelli, [Online]. Available: https://moscatelli.it/en/products/pannello-solare-off-grid-200w-spb200-42v?_pos=2&_sid=5d004804f&_ss=r. [Accessed May 2024].

[26] "Greencell.global," Green Cell, [Online]. Available: https://greencell.global/en/solar-inverters/4548-green-cell-solar-inverter-off-grid-converter-with-mppt-solar-charger-24vdc-230vac-3000va3000w-pure-sine-wave.html#specification. [Accessed May 2024].

[27] "milesolar.com," Mile Solar Company, [Online]. Available: https://milesolar.com/products/39/1kw-hybrid-solar-power-inverter-with-mppt-controller-30a-60a. [Accessed May 2024].

[28] Shenzhen Gitenno Technology Company, [Online]. Available: https://www.alibaba.com/product-detail/3kw-3kva-voltronic-power-mppt-inverter_1601195253435.html?spm=a2700.shop_plser.41413.11.295c6dc8pZXSOo. [Accessed June 2024].

[29] "PXR," PXR Company, [Online]. Available: https://pxr.es/. [Accessed 2024].

[30] "NVidia.Developer," Nvidia, [Online]. Available: https://developer.nvidia.com/embedded/learn/get-started-jetson-nano-devkit#intro. [Accessed June 2024].

[31] L. H. a. G. Mauthe, "The Universal Power Electronics Based Distribution Transformer, an Unified Approach," in *IEEE PowerElectronics Specialists Conference (PESC)*, 2001.

[32] "UNIFLEX," UNIFLEX Project, 2013. [Online]. Available: http://www.eee.nott.ac.uk/uniflex/Project.htm.

[33] E. K. A. M. B. B. K. M. S. S. P. N. a. P. R. M. SimoesR. Roche, "Smart-Grid Technologies and Progress in Europe and the USA,," in *IEEE Energy Conversion Congress and Exposition (ECCE), Sep. 2011, pp. 38*.

[34] M. H. K. a. R. W. D. Doncker, "Single phase unity power factor control for dual active bridge converter," in *Conf. Rec. of the IEEE Industry Applications Society Annual Meeting (IAS 1993), Toronto, Canada, 2–8 Oct. 1993, pp. 909–916.*.

[35] C. Y. L. L. Z. D. Q. F. C. L. a. J. S. L. K. Wang, "Bidirectional DC to DC converters for fuel cell systems," in *Proc. of the IEEE Workshop on Power Electronics in Transportation, Dearborn, MI22–23 Oct. 1998, pp. 47–51.*.